AD-774 140

CHALCOGENIDE GLASSES FOR HIGH ENERGY LASER APPLICATIONS

A. R. Hilton, et al

Texas Instruments, Incorporated

Prepared for:

Office of Naval Research
Advanced Research Projects Agency

January 1974

AD - 774140

DOCUMENT CONTROL DATA - R & D

(Security classification of title, body of abstract and indexing annotation must be entered when the overall report is classified)

1. ORIGINATING ACTIVITY (Corporate author)	2a. REPORT SECURITY CLASSIFICATION
Texas Instruments Incorporated Central Research Laboratories 13500 North Central Expressway Dallas, Texas 75222	UNCLASSIFIED
	2b. GROUP --

3. REPORT TITLE

Chalcogenide Glasses for High Energy Laser Applications

4. DESCRIPTIVE NOTES (Type of report and inclusive dates)

Technical Report No. 1, 1 May 1973 through 31 December 1973

5. AUTHOR(S) (First name, middle initial, last name)

A. R. Hilton
D. J. Hayes
M. D. Rechtin

6. REPORT DATE	7a. TOTAL NO. OF PAGES	7b. NO. OF REFS
January 1974	~~69~~ 78	23

8a. CONTRACT OR GRANT NO.	9a. ORIGINATOR'S REPORT NUMBER(S)
N00014-73-C-0367	
b. PROJECT NO.	08-74-06
c. ARPA Order No. 2443	9b. OTHER REPORT NO(S) (Any other numbers that may be assigned this report)
d. Program Code No. 3D10	

10. DISTRIBUTION STATEMENT

11. SUPPLEMENTARY NOTES	12. SPONSORING MILITARY ACTIVITY
	Advanced Research Projects Agency Washington, D. C.

13. ABSTRACT

Substantial reduction in the absorption at 10.6 μm is required before chalcogenide glasses can be used with high-energy CO_2 lasers. In this program, new methods for compounding high-purity TI-1173 glass (composition $Ge_{28}Sb_{12}Se_{60}$) and TI-20 glass (composition $Ge_{33}As_{12}Se_{55}$) were developed. At the present stage of purity, the absorption for TI-1173 at 10.6 μm is about 0.01 cm^{-1}. The absorption is dominated by the silica content of of the glass and can be lowered if the impurity is removed. The absorption for TI-20, however, is presently about 0.05 cm^{-1} and is dominated by a broad, low-level absorption centered about 12.8 μm. The absorption appears to be intrinsic, and little can be done to improve TI-20 further.

Concurrent to the purity effort, samples of glasses based on sulfur and selenium were carefully characterized to establish the interdependence between physical parameters and chemical composition. Relative to selenium, the sulfur-based glasses are shown to be harder, to have higher thermal conductivities and higher glass transition temperatures, and to have higher elastic moduli and smaller volume expansion coefficients. Selection of a sulfur composition will be made considering the absorption at 10.6 μm, the thermal stability of the glass, and the thermal change in refractive index.

DD FORM 1473
1 NOV 65

14. KEY WORDS	LINK A		LINK B		LINK C	
	ROLE	WT	ROLE	WT	ROLE	WT
Infrared transmitting glasses						
Absorption in chalcogenide glasses						
Interdependence of physical parameters for infrared transmitting glasses						
High-purity selenium-based glasses						

CHALCOGENIDE GLASSES FOR

HIGH ENERGY LASER APPLICATIONS

Contract No. N00014-73-C-0367

A. R. Hilton

D. J. Hayes

M. D. Rechtin

Texas Instruments Incorporated

Technical Report No. 1

January 1974

Sponsored by
Advanced Research Projects Agency
ARPA Order No. 2443

PROGRAM SUMMARY

Substantial reduction in the absorption at 10.6 μm is required before chalcogenide glasses can be used with high-energy CO_2 lasers. In this program, new methods for compounding high-purity TI-1173 glass (composition $Ge_{28}Sb_{12}Se_{60}$) and TI-20 glass (composition $Ge_{33}As_{12}Se_{55}$) were developed. At the present stage of purity, the absorption for TI-1173 at 10.6 μm is about 0.01 cm^{-1}. The absorption is dominated by the silica content of of the glass and can be lowered if the impurity is removed. The absorption for TI-20, however, is presently about 0.05 cm^{-1} and is dominated by a broad, low-level absorption centered about 12.8 μm. The absorption appears to be intrinsic, and little can be done to improve TI-20 further.

Concurrent to the purity effort, samples of glasses based on sulfur and selenium were carefully characterized to establish the interdependence between physical parameters and chemical composition. Relative to selenium, the sulfur-based glasses are shown to be harder, to have higher thermal conductivities and higher glass transition temperatures, and to have higher elastic moduli and smaller volume expansion coefficients. Selection of a sulfur composition will be made considering the absorption at 10.6 μm, the thermal stability of the glass, and the thermal change in refractive index.

TABLE OF CONTENTS

Preceding page blank

Table of Contents

(Continued)

LIST OF TABLES

vi

LIST OF ILLUSTRATIONS

LIST OF ILLUSTRATIONS

(Continued)

SECTION I

INTRODUCTION

Infrared transmitting glasses based on the chalcogens sulfur, selenium, and tellurium have been under investigation at Texas Instruments as optical materials since the fall of 1961. After several years of exploratory efforts, the glass program was transferred from the Central Research Laboratories into the user division, passing into a pre-production stage. Finally in 1968, one glass, TI-1173 (which has the composition $Ge_{28}Sb_{12}Se_{60}$), was incorporated into the design of a FLIR system, enabling the designer to color-correct (color refers to the wavelength range of operation, 8 to 14 μm) by pairing the optical elements with germanium. Since that time, the production and use of TI-1173 has been extensive, passing the ten tons mark in 1972. A second glass, TI-20 ($Ge_{33}As_{12}Se_{55}$), has reached a production stage and has found limited application as an external window and in prototype optics.

Major emphasis of the first production programs was technical feasibility; that is, the technical accomplishment of being able to compound and cast a nonoxide glass in much the same manner as optical glasses while maintaining adequate quality. Gradually, the increased production and use of FLIR systems led to demands for increased optical quality of the glass. The production methods improved, and the present quality is adequate for avionics systems as guaranteed through a set of quality assurance specifications. However, if one compares the avionics systems quality requirements to those set by the "High Energy Laser Window" problem, a two orders of magnitude reduction in absorption is required.

This background underlies the basic point of view adopted by the investigators in this laboratory in approaching the problem of how to prepare chalcogenide glasses better suited for use with the high energy CO_2 laser emitting at 10.6 μm. The first goal is to establish the absorption limit for selenium-based glasses

through increased purity Since we have never really tried to prepare these materials in exceptionally pure form, we approached the purity problem as we would any other semiconductor materials preparation problem. The second goal of this program is to select one or more new glass compositions to obtain glasses with properties better suited for application with CO_2 lasers. To guide the selection of new glass compositions, an effort concurrent to the increased purity program was started to establish the interdependence of the physical parameters important to the use of the material in infrared optics. The goal is to select a sulfur-based glass composition with better physical properties and a refractive index that is unaffected by temperature.

SECTION II

EVALUATION METHODS

A.   Trace Impurity Evaluation

Materials transparent out to 14 µm are almost always plagued by trace oxide impurities introduced during the preparation step or appearing in the beginning reactants. Ironically, most trace analytical methods have been developed for metallic impurities which affect the transport properties of crystalline semiconductor solids rather than for the nonmetallic impurities.

1.   Emission Spectrograph

Trace metallic impurities in solids are generally determined in this laboratory using a Baird Atomic GX-1 three-meter grating (30,000 grooves/in.) emission spectrograph. High purity Poco Graphite electrodes are used, leading to a detection limit of 0.1 to 10 ppm/weight for most common metallic elements. Trace anion impurities such as Cl^-, Br^-, or OH^-, along with negative elements such as S, Se, or Te, are not ordinarily detected (unless they are present as a major constituent).

2.   Solids Mass Spectrograph

The laboratory is also equipped with an AEI MS7 solids mass spectrograph. Detection limits for most metallic elements are much lower, in the low parts/billion range. However, the samples must be fabricated in the form of small electrodes so that an arc can be passed between them. Ions from the arc are drawn into the mass analyzer portion of the instrument and allowed to strike a photographic plate. Good results are not obtained unless the electrode material is slightly conducting (< 100 ohm cm). Also, major contributions to the ion source come from the surface of the sample, usually oxygen and carbon. For this reason, the method is not recommended for bulk oxide or carbon analysis.

3. Infrared Absorptions by Oxides

Semiconductor solids transparent in the infrared show absorption characteristic of oxide impurities present within the bulk, classic examples are silicon (9.5 μm) and germanium (11.6 μm).[1] The magnitude of the absorption coefficient can be used to estimate the concentration of oxygen present.[1] The measured transmission of the reactant germanium can then be used to estimate the beginning oxygen concentration.[1] Bands characteristic of oxides in selenium have also been reported in the literature.[2] However, neither antimony nor arsenic, the other reactants, transmit in the infrared.

4. Neutron Activation Analysis

Recently,[3] workers using activation analysis techniques have been able to go well beyond the sensitivity limit (2 ppm) of the infrared transmission method in silicon down to the low ppb range. The method used is general and can be applied to other solids, provided proper samples can be obtained and an etch suitable for removal of surface oxides is employed. The methods were developed by the staff of the Center for Material Trace Characterization, Department of Chemistry, Texas A & M University.

B. Optical Evaluation

1. Infrared Transmission

Two optical null double-beam infrared spectrophotometers are used to measure infrared transmission of polished glass samples: a Perkin-Elmer Model 337 and a Perkin-Elmer Model 221, with transmission scale expansion. According to the manufacturer, both instruments will yield better than 1% transmission accuracy. However, for low absorption - high refractive index materials, this accuracy cannot be maintained. To measure an appreciable change in transmission, the samples must be thick, which leads to an increase in the optical path on the sample side. Consequently, the optical image of the globar source on the active area of the detector is defocussed, resulting in an inaccurate comparison of I to I_o. The degree of the inaccuracy is a variable, depending on the instrument design and on the refractive index and the thickness of the sample.

The Perkin-Elmer 337 is used for convenience and covers the range from 2.5 to 25 μm. Transmission is recorded on standard paper which is easily stored in looseleaf notebooks for reference. However, the 337 is a grating instrument and yields more accurate transmission data at wavelengths past 12 μm than does the Perkin-Elmer 221 (with NaCl interchange). The Perkin-Elmer 221 has a relatively long focal length optical system (long relative to the Perkin-Elmer 337) and therefore yields more accurate transmission values for the thick glass samples. The expanded transmission scale feature (5X, 10X, and 20X) is also an advantage in trying to estimate the absolute transmission for a sample when the absorption is a few percent or less. However, the scale factors quoted by the manufacturer must be checked by comparing transmission values for the same sample in low absorption regions recorded while using 1 x %T 5 x %T, etc., so that the real values for 5, 10, or 20 can be calculated. The ability to calculate the absorption-free transmission values from the precise five-number refractive indexes for the TI-1173 and TI-20 glasses has been very helpful in this program. In this way, the validity of the high transmission - very low absorption values can be judged.

A third source of transmission values will be derived from the use of a Perkin-Elmer E-1 monochromator. At present, a globar source is used with a thermocouple detector and a Perkin-Elmer lock-in amplifier. Improvement of the system is planned. The usefulness of this system is its better spectral resolution, particularly at longer wavelengths, and the ability to use dewars for transmission as a function of wavelength. The disadvantages are that the measurements must be made single-beam, point by point, and that there is an inherent limitation in using an electrical signal instrument as opposed to an optical null.

2. Laser Calorimetry

The most convenient method used for measuring low-level absorption by most investigators for 10.6 μm values is the laser calorimeter. A diagram of the system used in this laboratory is shown in Figure 1. The laser is a single-mode, 50-watt Perkin-Elmer #6200. Incident powers from 7 to 15 watts have been used. The sample can be removed from the path for power settings.
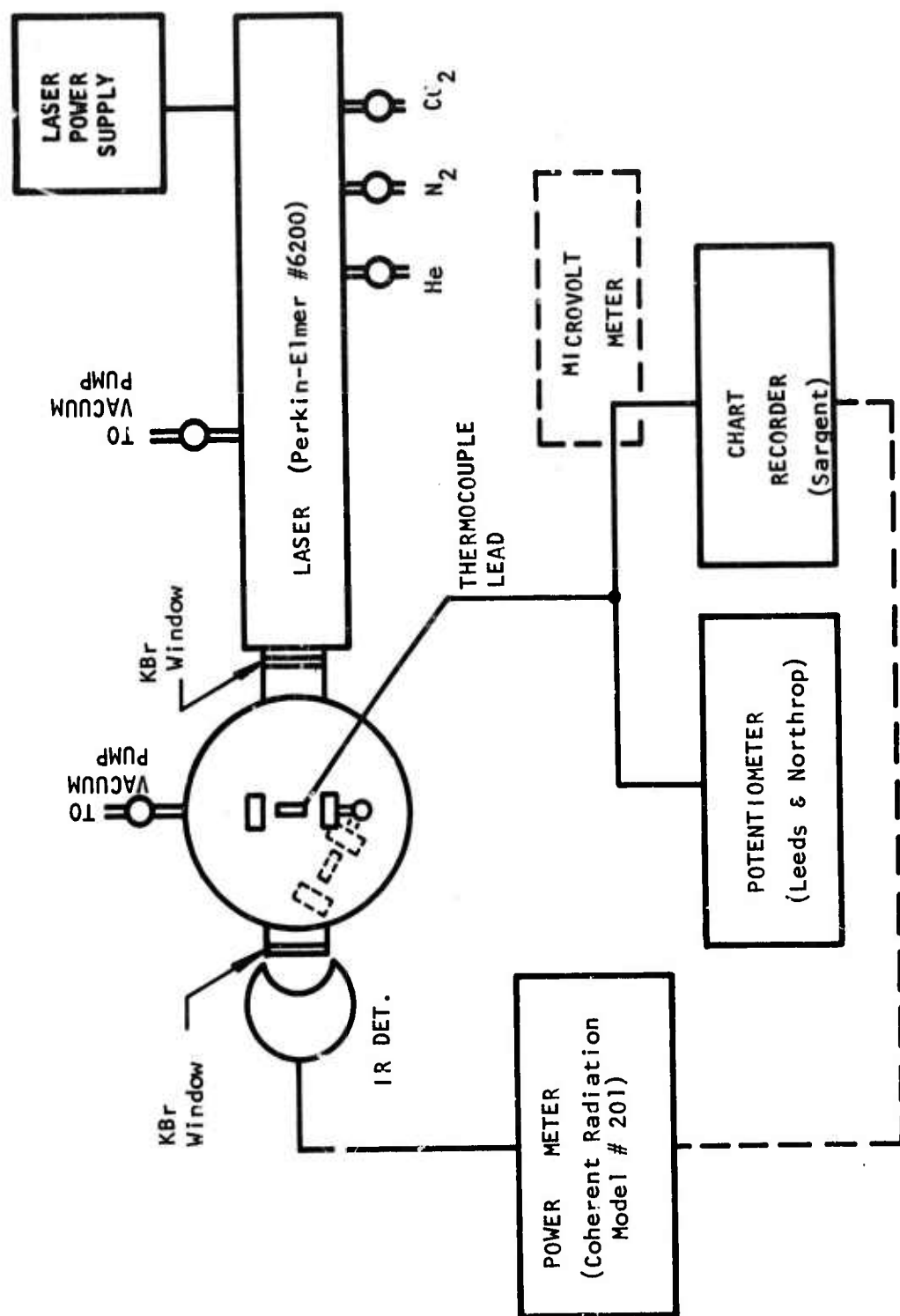
Figure 1 Laser Calorimetric System

Measurements have been made both in air and under reduced pressure, with results in air giving slightly lower values. The power meter is new and agrees well with another power meter manufactured by the same company that was recently returned for calibration. Both the adiabatic technique as described by Hass[4] and the steady state technique[5] have been used, giving comparable results. At present, the steady state method is used for convenience. Samples are core-drilled about 1.1 inch in diameter and about 0.5 to 0.6 inch thick. They have a small 40-mil hole cavitroned in the side for a 5-mil diameter copper-constantan thermocouple. The hole is about 0.1 inch deep and is filled with "heat sink" compound to promote good heat transfer. The faces of each sample are polished plane and parallel using a Buhler Vibromet polisher and the usual alumina fine-grain polishing compounds.

3. Infrared Microscopy

A Research Devices Incorporated Model D infrared microscope has been of invaluable assistance in evaluating the quality of the infrared glass samples. The microscope is equipped with a Polaroid camera so that a permanent record can be made of infrared (~ 1.1 μm) images up to 430X taken in transmission or with reflected light. The instrument has been used to verify the removal of carbon particles from the glass or to investigate the possibility of crystallite formation.

4. Striae

The problems encountered with striae in glass produced at Texas Instruments were discussed earlier[6] with regard to both the "striaescope" used in detection and the casting method cause of striae. Since that time, the optics department at Texas Instruments has designed and constructed a new long focal length optical system which has at least an order of magnitude greater sensitivity to striae than the previous system. At the same time, a "bottom hole" method for casting glass was developed which has led to an estimated order of magnitude decrease in the striae level in cast plates (the test is somewhat subjective). In the new method, molten glass pours from a tube in the bottom of the heated container

filled with glass. The decreased striae level is illustrated in the before and after photographs shown in Figure 2. Both photographs were made using the new striae optical detection system.

5. Optical Transfer Function

Previously,[6] the computerized system designed and built by Tropel, Inc. for measuring the effect on optical transfer function (OTF) of infrared glass plates was described. The system measures the change in performance of a high resolution infrared optical system when a flat, polished cast-glass plate is placed in the optical path (a collimated light portion). The specification for TI-1173 previously[6] had allowed a 15% degradation (85% MTF) at the frequency point of 10 lines/mm. With the improved striae situation, the specification on cast TI-1173 plates has been increased so that now only 6% degradation (94% MTF) is allowed at the 10 lines/mm point. High-quality,[7] large-grain polycrystalline germanium is the only other infrared optical material useful with avionics systems tested in our image evaluation laboratory that can meet this specification.

C. Physical Evaluation

1. Density

The density was determined by the Archimedean method using an Ainsworth Microbalance and distilled water as a medium.

2. Thermal Expansion and T_g

A quartz tube dilatometer was used to obtain both the coefficient of thermal expansion ($\Delta L/L$) and the glass transition temperature (T_g). The equipment used was a Daytronic Model 300D Transducer Amplifier-Indicator with Type 71 plug-in in conjunction with a Daytronic Linear displacement transducer. The system was capable of operating from room temperature to approximately $1000^\circ C$. A typical curve taken on an X-Y recorder is shown in Figure 3. The method used to define T_g is indicated in this figure. Use of the differential thermal analysis method (DTA) was discontinued when it was found that residual strain in polished glass samples significantly affected the measured results.
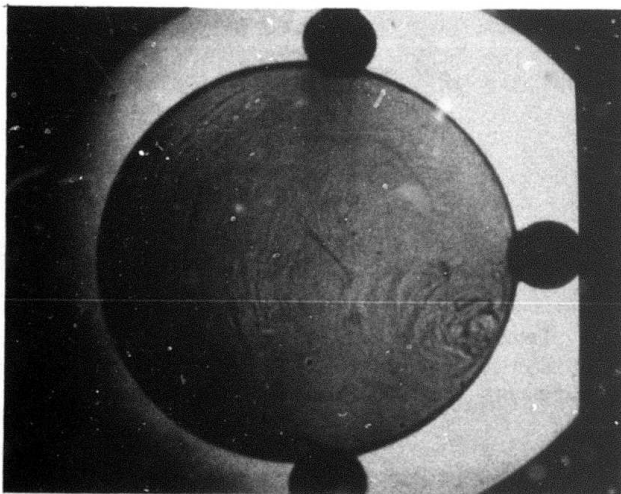
1173 STRIAE STANDARD
CAST: APRIL 1971
(OLD CASTING METHOD)
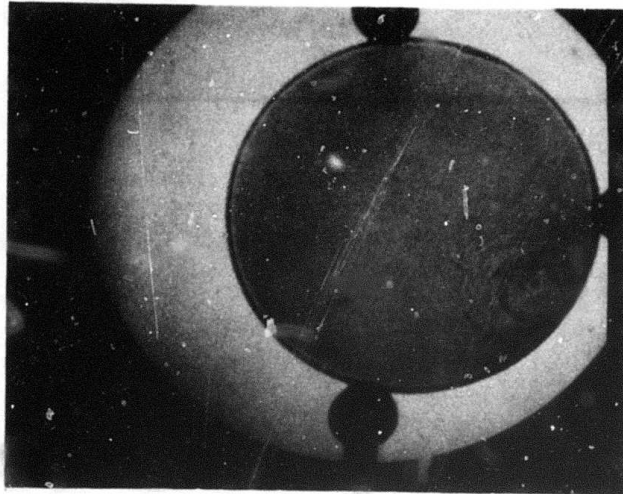
BLANK: 34173
CAST: 6/11/73
(BOTTOM CAST)

Figure 2 Striae Comparison of 5 1/2-Inch Diameter TI-1173 Blanks

9
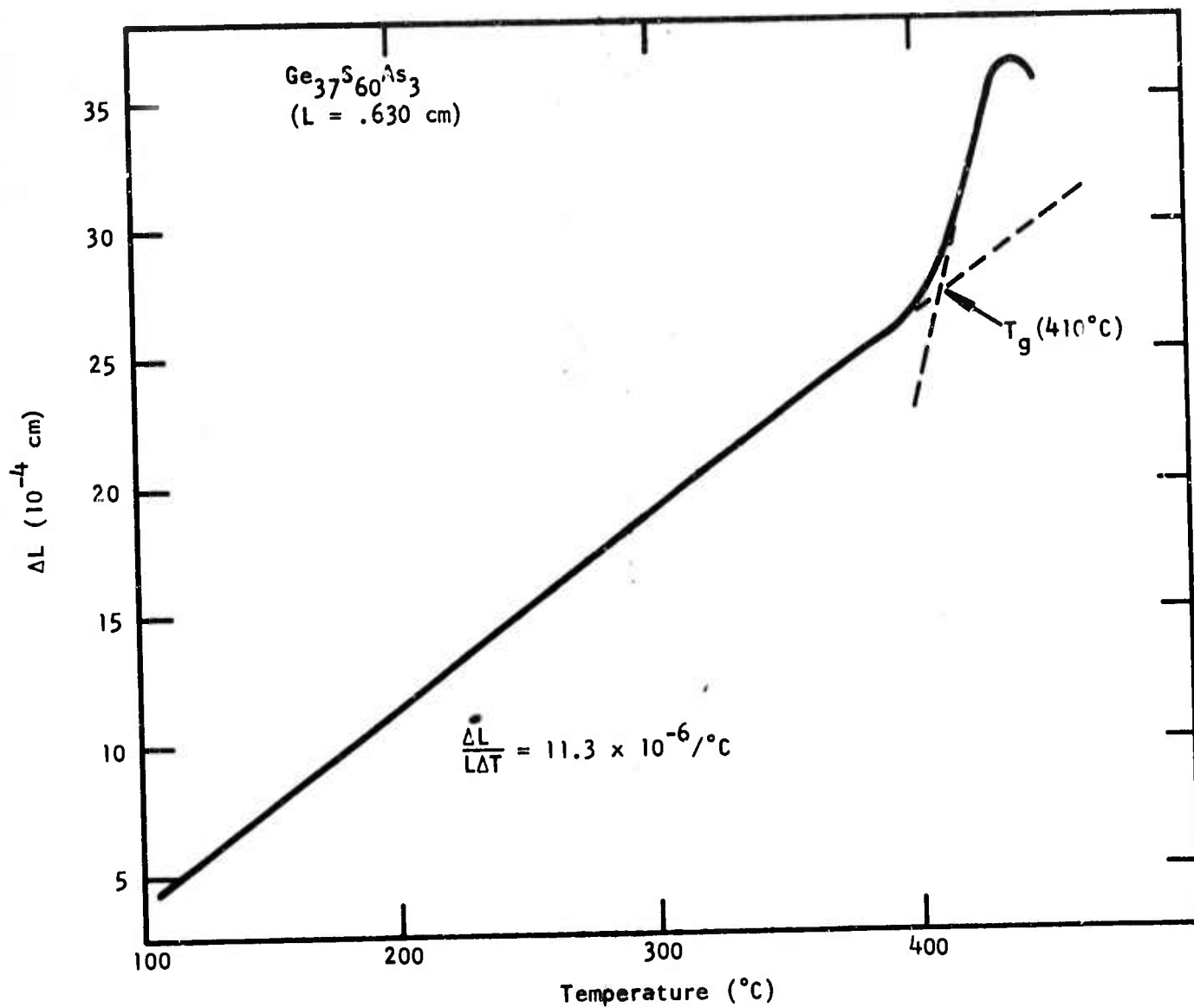
Figure 3   Dilatometer Measurement of Glass Transition Temperature (T_g)

10

3. Hardness

The microhardness was measured using a Leitz Miniload Hardness Tester and a knoop diamond. The knoop hardness (H) is given by the relation

$$H = 14.23 \times 10^3 \, P/d^2 \quad ,$$

where P is the applied load in grams and d is the length of the indentation in μm. The hardness values for TI-1173 as a function of load are given in Table I.

Table I

Hardness Values for TI-1173 as a Function of Load

Load (gm)	Hardness (knoop)
25	161
50	157
100	153
200	144

Since the hardness value determined with the above equation is a function of the load, it is important to state the value of the load when reporting hardness values. For the data in Table I the load was applied for 30 seconds. Times of 10 seconds or less give hardness values larger than those in the table. It is difficult to use longer times for these relatively soft materials because even small mechanical vibrations will drive the indentor deeper into the glass.

4. Thermal Conductivity

The thermal conductivity of the sulfur- and selenium-based glasses was measured using a Thermal Comparator Model 100 obtained from McClure Park Corporation. This instrument works on the principle that the rate of cooling experienced by the tip of a heated probe upon contact with the surface of the sample can be related to the thermal conductivity when the system has been calibrated with known thermal conductivity standards. The quoted reproducibility is ± 2% or better, and the quoted accuracy is given as ± 5% or better on well-characterized surfaces.

11

The thermal conductivity of TI-1173 and TI-20 glasses was also measured as a function of temperature from -100°C to +200°C. The axial-flow steady state method was used. A diagram of the system is shown in Figure 4. Good thermal contact was ensured by using heat sink compound on both the heat source and the heat sink sides of the samples. Heat leaks were minimized by using Union Carbide super-insulation in conjunction with a vacuum better than 10^{-5} Torr.

5. Elastic Moduli

The Young modulus (E) and the shear modulus (G) were determined on a series of selenium-based and sulfur-based glasses by measuring the velocity of both longitudinal (v_L) and shear (v_S) sound waves. Knowing these velocities and the density (ρ) of the material, E and G were calculated from the following relations:

$$E = 2G(1 + v), \quad G = \rho\, v_S^2 \quad,$$

where Poisson's ratio (v) is given by:

$$v = \frac{1}{2} - \frac{1}{2}\left(\frac{v_S^2}{v_L^2 - v_S^2}\right) \quad.$$

The sound velocities were measured by the pulse-echo method using a Sperry Attenuation Comparator with a 0 to 100 μsec digital delay. The absolute accuracy of such a system is slightly better than 1% for the velocity measurements. This would give approximately 2% accuracy in G and slightly less than this for E.

6. Rupture Modulus

Although the fracture behavior of glass is an extremely complicated problem, some basic understanding does exist due to the large amount of experimental work on oxide glasses. A few of the most important experimental observations[8] are summarized below.

● For a homogeneous glass the fracture is always of a brittle nature, starts at the surface, and is initiated by tensile stress.
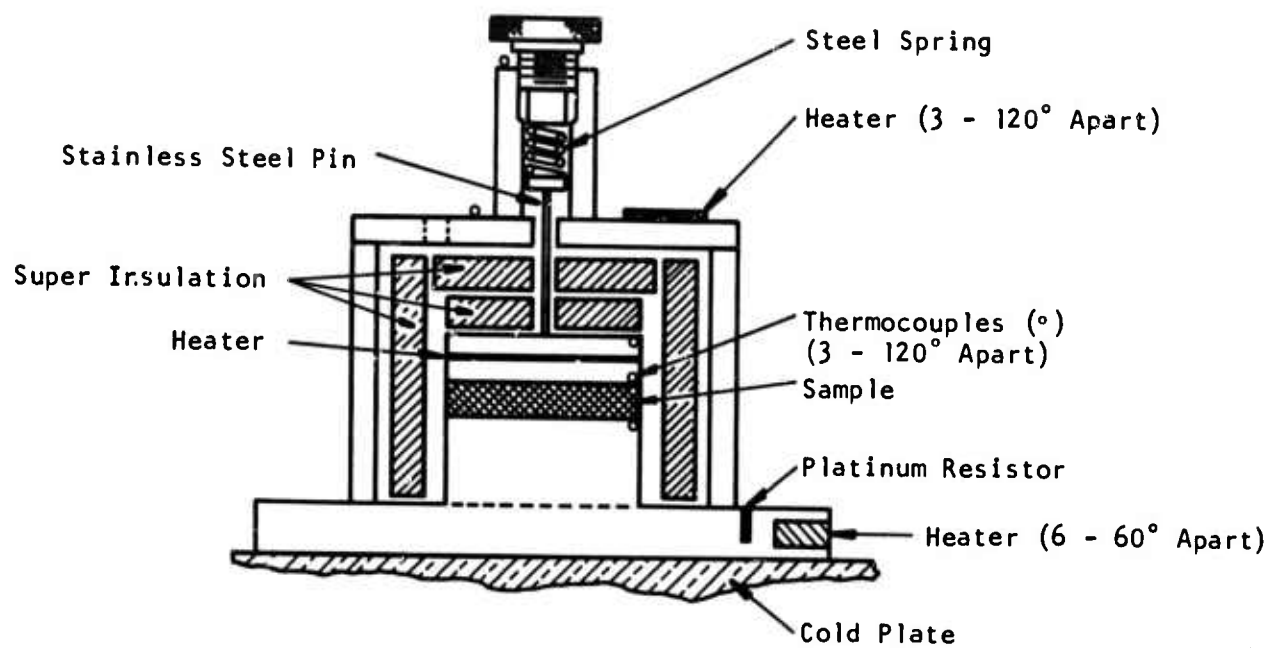
Figure 4   Thermal Conductivity Apparatus

13

• The theoretical strength of a glass is calculated to be 100 to 1000 times the observed stren.th. The observed strength is believed to be determined by the applied tensile stress at the most severe flaw present in the stressed region. The results of rupture modulus test show considerable scatter.

• The observed rupture modulus varies inversely with the area under stress. This is based on the idea that the probability of a critical flaw existing in the area under maximum stress increases as the area increases, implying that the observed rupture modulus would be larger for three-point loading than for four-point loading. Also, one would expect large plates to rupture at still lower stress.

It should be pointed out that to some degree all three of these observations apply not only to glasses but also to other brittle materials being considered for the laser window problem.

Most of the testing performed so far at Texas Instruments has been done using either three-point or four-point loading methods on bar samples. Because of the brittle nature of these materials, a self-aligning fixture was used. One problem in testing bar samples arises from the large number of edge failures. To eliminate this problem and also to test large plates, a fixture has been designed to test circular glass plates.[9] This system uses concentric rings to apply the load in such a way that the stress at the edges is less than 50% of the maximum stress. Eliminating edge failures and testing large areas should provide results that are more representative of the real properties.

SECTION III

GLASS PREPARATION

A. Production Methods

1. Reactant Purification

The stated purity of reactants used in compounding glasses may be as high as six-nines. However, the purity figure does not include surface oxides. The surface oxides are removed by sublimation from the heated reactant either in flowing gas or under reduced pressure. Table II shows some values obtained using the solids mass spectrograph, the accuracy of which (as pointed out earlier) is adversely affected by surface oxides with as-received reactants. Infrared transmission of polished samples of the germanium indicate the actual bulk value was 0.2 to 0.3 ppm. Infrared transmission of a polished amorphous selenium sample showed no detectable selenium oxide absorption according to the absorptions reported by Vasko.[2] The antimony (and arsenic) cannot be tested by infrared transmission because of their metallic nature.

All reactants (except germanium, which is used in bar form) are treated in a similar manner to sublime the volatile surface oxides from the surfaces. Sublimation is carried out in cleaned glass or quartz tubes using flowing gas or reduced pressure to promote the separation. Temperatures used are 300°C for selenium, 700°C for antimony, and 600°C for arsenic. Care is taken to minimize exposure of the purified reactants to moist air before use. The reactants are used almost immediately after purification.

2. Compounding

Quantities large enough for a 4 to 5 kgm batch of glass are weighed out; broken up using a large mechanical grinder; and placed in large, clean, high-purity quartz tubes. The entire amount is heated slightly (~ 200°C) and sealed off at reduced pressure. The tubes are placed in a rocking furnace, brought up to 800°C, and reacted for about 18 to 24 hours. Air-quenching from 575°C is used.

TABLE II

OXIDE IMPURITY LEVEL IN REACTANTS AS
DETERMINED BY THE SOLIDS MASS SPECTROGRAPH

Reactant	Oxide Impurity Level
Ge	135 ppma
Sb	170 ppma
Se	100 ppma

3. Casting

Enough bulk pieces of glass are placed in a large resistive-heated, beaker-shaped furnace to provide glass for the cast plates. The furnace is in a large metal chamber which has been filled with forming gas (10% H_2, 90% N_2). The glass is melted and stirred from above at a temperature of about 600 to 650°C, cooled down to 575°C, and cast into a heated mold. The oxide impurity level for the cast glass is found to increase slightly from that of the compounded glass due to increased exposure. The production area oxide impurity level as estimated by the infrared transmission measurement[6] at 13 µm averages 3 to 4 ppm.

4. Annealing

Each cast plate is annealed using a programmed schedule that reaches to within a few degrees of the T_g and then cools very slowly. The entire process takes about 48 hours.

5. Evaluation

Each plate is numbered, and a permanent record of its evaluation is kept. The plate is polished on both sides in the glass production area (not the optics shop) and checked for transmission. A loss greater than 2% for a 0.5-inch thick plate is a failure. The plate is examined for striae, and a Polaroid photograph is made of the television display for a permanent record. If the plate is judged to be of good quality, it 's sent to the image evaluation laboratory for the OTF test. Slumping of the glass is carried out only if all tests are passed.

B. New Methods

• Combination of Purification and Compounding Steps

Examination of the steps followed in the production process indicated that exposure to air after purification and during the casting operation was leading to an increase in the oxide concentration. A combination of all three steps was the basis for the methods outlined in the proposal for this program. However, it was soon realized that casting was a problem separate from the

17

purity problem, a problem that could be overcome (in view of the recent improvement in the production area) whenever large plates were required. It was therefore decided to restrict our attention to 1 kgm quantities and to cut and polish small samples from the 1 kgm boule for evaluation. The procedure followed is depicted in the following figures.

Figure 5 diagrams the procedure followed in purifying the reactants. Three (or two) separate chambers are provided. The two outside chambers contain selenium and antimony (or arsenic). The center chamber contains the germanium and serves as the compounding chamber. Porous quartz frits are used to filter particulate matter when a reactant is distilled into the center chamber. This step is absolutely essential for the selenium since (as we reported previously) the as-received material has been shown to contain amorphous carbon.

Prior to placing the reactants in the chambers, the chambers were etched, dried, and placed in their respective furnaces. With a dry, oxygen-free gas (generally hydrogen) flowing through, all three chambers and the frits are heated to 800°C and flushed overnight to drive moisture from the quartz. The chamber is then cooled with an inert gas present (nitrogen or helium). The reactants are added, and the surface oxide treatment is begun. A temperature of 300°C is used for the selenium, 700°C for the antimony and germanium, and 350°C for the arsenic. The process is run overnight, covering a period of 16 to 18 hours.

The seal-off procedure and the distillation are depicted in Figure 6. The ends of the reactant chambers are pulled off. All the chambers are evacuated using a tube in the center reactor chamber. The reactants are kept hot ($\sim 300°C$) and the pressure is lowered to a range of 1 to 5×10^{-4} Torr using a diffusion pump trapped with liquid nitrogen. The next step is to seal off the reaction chamber while the reduced pressure is maintained. After seal-off, the reactants are distilled through the frit into the center chamber. Care is taken to use temperatures that do not produce a vapor pressure much above atmosphere. The temperature for selenium and arsenic is 650 to 700°C. Distillation for antimony required a temperature of 1000°C and was extremely slow. The
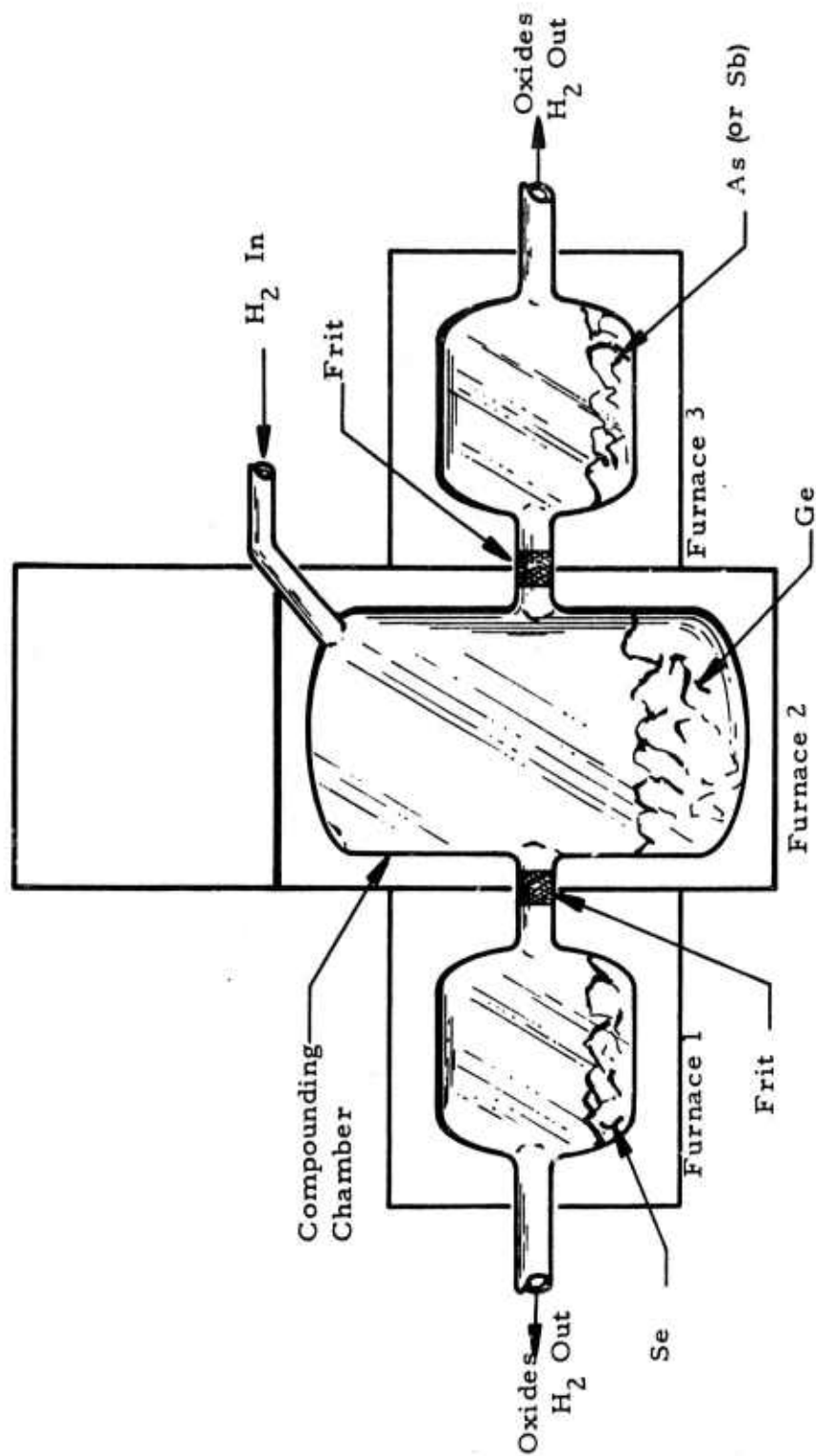
18

Figure 5   Process for Reactant Purification

19
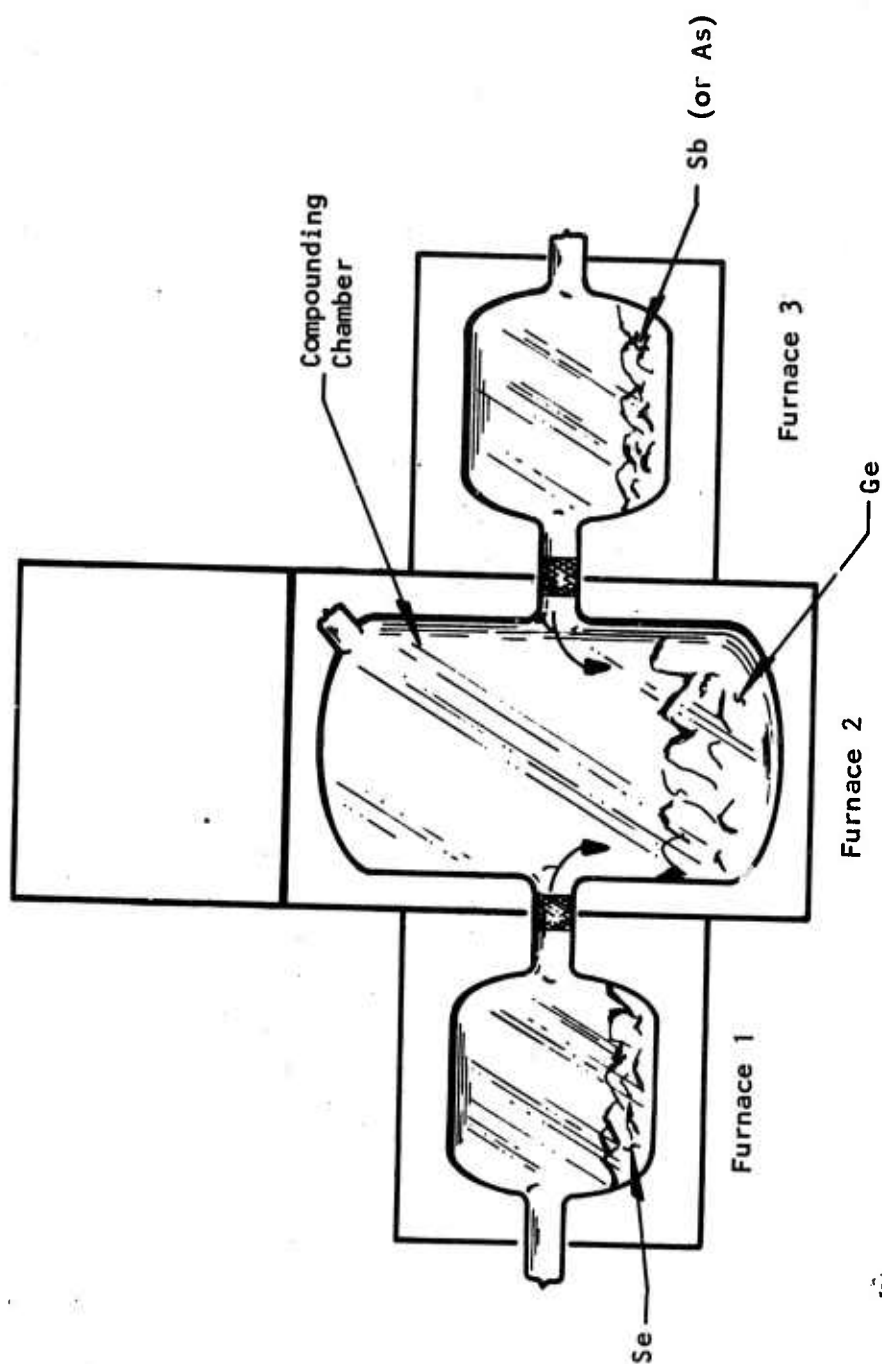
Figure 6 Distillation of Reactants

Compounding Chamber

Sb (or As)

Ge

Se

Furnace 1

Furnace 2

Furnace 3

20

reaction chamber which is not heated during the distillation step serves as a cooled surface for condensation of the reactant vapors. When the distillation is complete, the side chambers (or chamber) are pulled off using the hydrogen torch without losing the reduced pressure.

The final step in the glass preparation is shown in Figure 7. The compounding chamber is placed in a rocking furnace, raised slowly to compounding temperature (700 to 800°C), and rocked for periods of from 12 to 48 hours. Quenching of the glass is carried out from a temperature of 575°C. The rocking action is maintained while the molten glass is cooled to this temperature. Air-quenching is accomplished by turning off the power, opening the furnace (a split type), and blowing room air onto the quartz chamber using a hand-held blower. The furnace is placed in a near-upright position during this process to allow the glass to flow into the bottom of the chamber to provide a cylinder of glass. The process is continued until the glass sample and furnace elements reach an equilibrium temperature of 250 to 275°C. The furnace is then closed, and the glass is allowed to anneal at 275°C for 6 to 8 hours. The final step is to cut off the power to the furnace and allow a slow cool-down for glass and furnace to room temperature overnight. The entire operation for compounding 1 kgm of glass is lengthy, requiring two to three weeks from start to finish.

Molten Glass

Figure 7 Glass Compounding
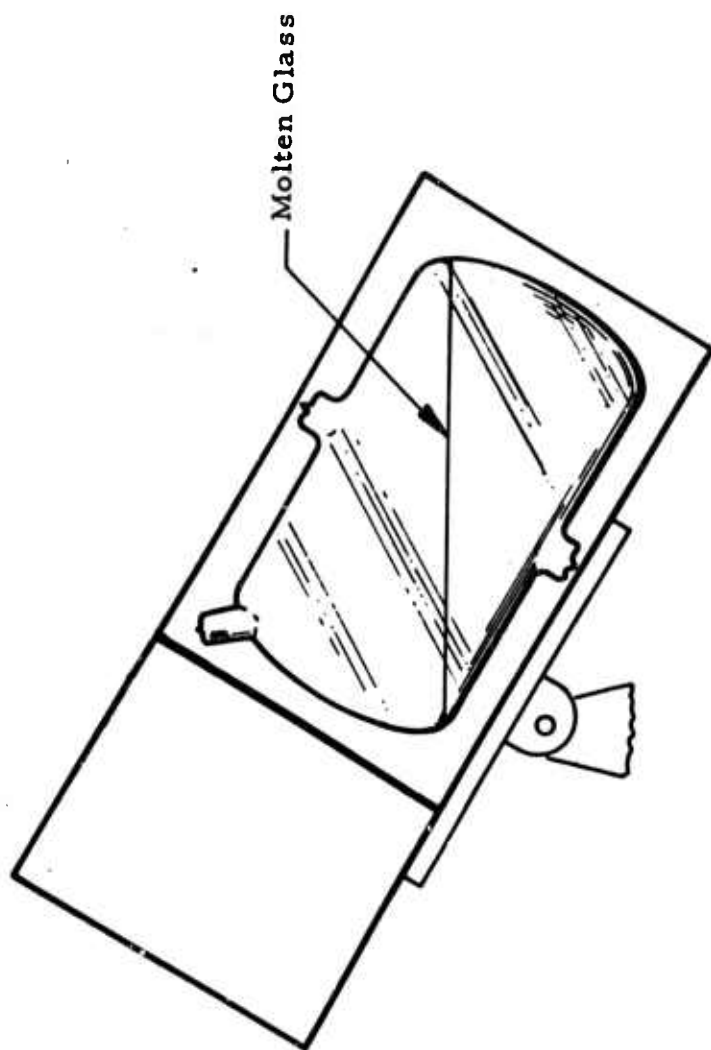
SECTION IV

RESULTS

A. TI-1173

The first attempts to use the compounding methods described to prepare TI-1173 were made prior to the beginning of this contract. The three-chamber method (described previously) was used, but it was found that antimony distillation through a frit was impractical. The amount of antimony required (178 gm) was distilled at $\sim 1000°C$ for about eight days, and no residue was left in the antimony container. It was therefore decided that in future preparation of the Ge-Sb-Se glass, only two chambers would be used, and the antimony would be placed in the center chamber along with the germanium. Both were treated for surface oxide removal at the same time. A trace amount of aluminum (~ 5 mgm) was added to the center chamber, as well.

The first good quality batch of TI-1173 that was prepared using the new methods and completely evaluated was run number 92. The calculated absorption coefficient as a function of wavelength is shown in Figure 8. The upper curve added to the diagram represents what is considered to be good production-area cast TI-1173. Note that the magnitude of absorption at about 13 μm is 0.6 to 0.7 cm^{-1}, while it is 0.2 cm^{-1} for our glass as a result of the addition of 5 ppm Al (none is added in the production area).

The measured laser calorimeter values have been added to the curves. TI-1173-92 was also evaluated by workers in other laboratories. The Naval Research Laboratory value (NRL, Dr. Marvin Hass) at 10.6 μm was 0.01 ± 0.005 cm^{-1}. The Catholic University values (C. U., Macedo and Moynihan) were 0.007 to 0.01 cm^{-1} at 10.6 μm and 0.0035 cm^{-1} at 10.15 μm. Our own value at 10.6 μm is 0.012 cm^{-1}, taken using the steady state method.

The dashed lines are values calculated using the expanded scale feature of the Perkin-Elmer 221. The method used is to estimate the increase in transmission from a point where a reasonably accurate value of the absorption coefficient
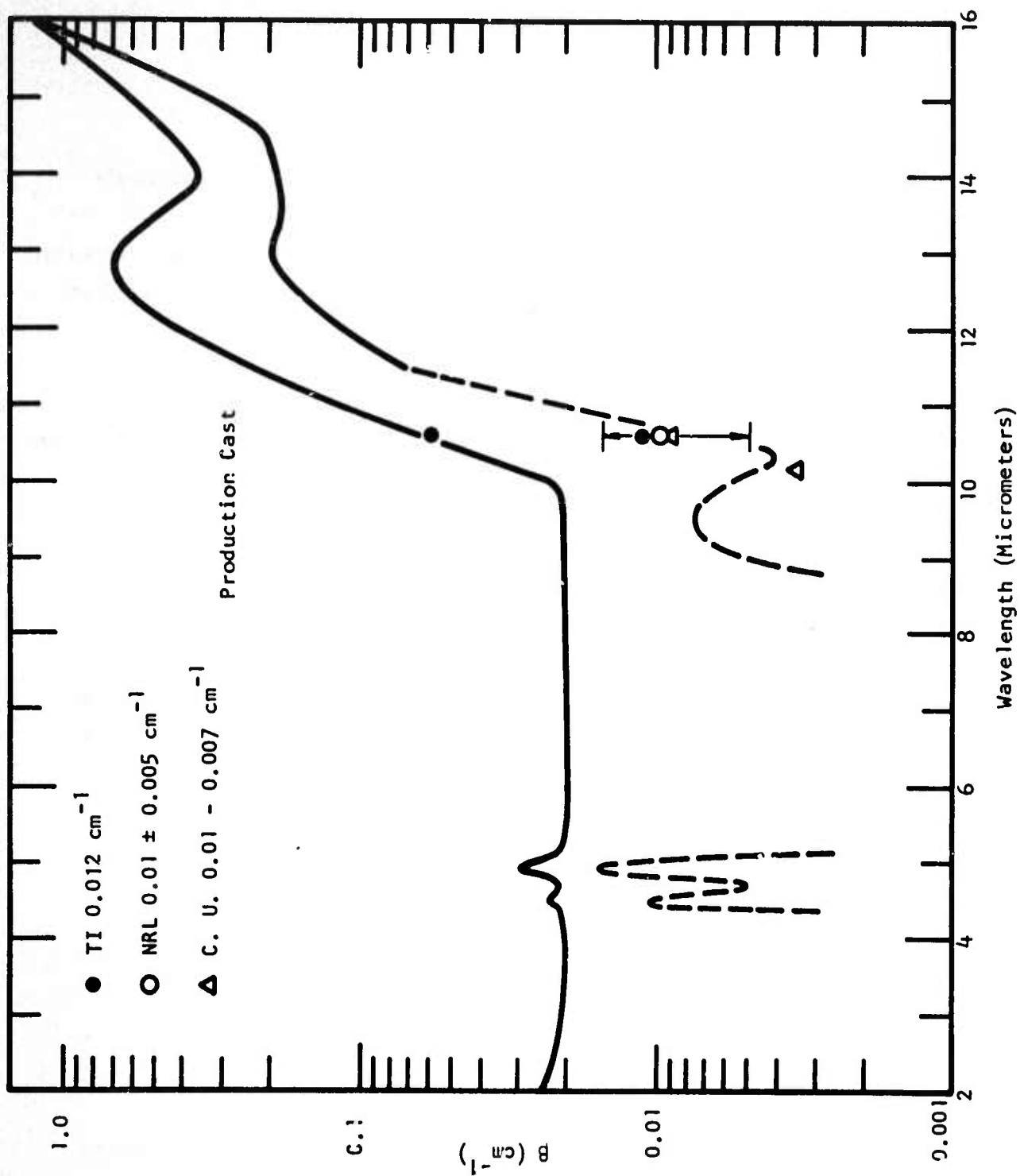
23

Figure 8 Absorption Coefficient as a Function of Wavelength for TI-1173-92

can be calculated. The estimate is based on transmission measurements made with samples of two different thicknesses in an absorbing region. For these glasses the point was 11.5 µm using the Perkin-Elmer 337. The solid curve represents this determination. The dashed curve represents the estimated values from the Perkin-Elmer 221. As mentioned previously, the absorption-free transmission calculated using the precise refractive index measurements is an important means of verifying the validity of the values. Good agreement between laser calorimeter values and calculated values is obtained.

Two more features of the curve should be mentioned. First, a low-level absorption at ~ 9.4 µm is observed. After that absorption, the short wavelength region from 5 to 9 µm appears to reach the 0.001 to 0.002 cm^{-1} level. The two absorption peaks at 4.56 µm and at 4.96 µm presumably are due to dissolved gases. They are variable in magnitude and in intensity relative to one another. The two gases suspected of being the cause are H_2Se and H_2O. The magnitudes of the absorptions are again estimated by comparing 1X and 7X transmission scans. The presence of these two bands reflects the use of hydrogen during purification, perhaps the presence of residual dissolved gases in the reactants, and probably the evolution of H_2O from the quartz during the seal-off process.

The method produced low absorption glass. The next step would be to try to increase the purity further. Examination of previous reports and notebooks revealed that the only constituent that had not been varied relative to purity was germanium. Six-nines selenium and antimony had been used in this glass and had been used in previous batches in the production area with no noticeable difference in absorption from glasses prepared with reactants of slightly lower purity. We decided to prepare glasses in which the known oxygen concentration was lower than the 0.2 to 0.3 ppm level of the first deposited germanium generally used. Also, single crystal germanium, because it had been melted in a reduced pressure environment, should contain a smaller amount of dissolved gases. Arrangements were made to purchase germanium with 30 ppb and 2.3 ppb oxide.[7] The design of the compounding apparatus was such that the germanium and antimony were placed in the compounding chamber without being broken to avoid exposure of the fresh

surfaces to air. This required that a wide-mouth chamber be constructed and another chamber-end with a narrow pump-out tube sealed on the end after the reactants were added. To avoid hydrogen contamination, the oxide removal step was carried out while the reactants were heated under reduced pressure in both chambers. The distillation of selenium into the compounding chamber was carried out, the chamber sealed off, and the glass reacted in the usual manner. Absorption as a function of wavelength for the glass compounded using the 30 ppb oxide germanium, TI-1173-107, is shown in Figure 9. The laser calorimeter value obtained in our laboratory, 0.019 cm^{-1} at 10.6 μm, is shown as a single dot. Note the close agreement with our calculated value. As before, the dashed line represents the values obtained using the expanded scale transmission values. Note that improvement is not observed. Also, the absorption at 9.4 μm and the gas absorptions at 4.54 μm and 4.96 μm have increased. The level of absorption just barely breaks the 0.01 cm^{-1} value at 7 to 8 μm.

Results obtained with the 2.3 ppb oxide-containing germanium were even worse. A plot obtained for TI-1173-109 is shown in Figure 10. Again, close agreement between the calculated absorption and the laser calorimeter value, 0.024 cm^{-1} at 10.6 μm, is obtained. The absorption at 9.4 μm has again increased while the two absorptions due to the dissolved gases have diminished. The general level of absorption for the glass is 0.01 to 0.02 cm^{-1} in the 5 to 8 μm range.

B.   TI-20

The same procedure was followed for TI-20 glass except that the arsenic was placed in the same chamber as the selenium. Oxide removal was conducted at a little higher temperature (350°C) using hydrogen. The germanium was the semiconductor grade germanium (0.2 to 3 ppm oxide) normally used, while the arsenic was the same six-nines pure material used in the production area for high purity GaAs. Complete distillation through the double frits required 700°C maximum temperature. The calculated absorption as a function of wavelength for the glass, TI-20-98 is shown in Figure 11. The top curve, added for comparison, represents results obtained from a piece of good quality, cast production area material. The 10.6 μm laser calorimeter values, 0.054 cm^{-1} for
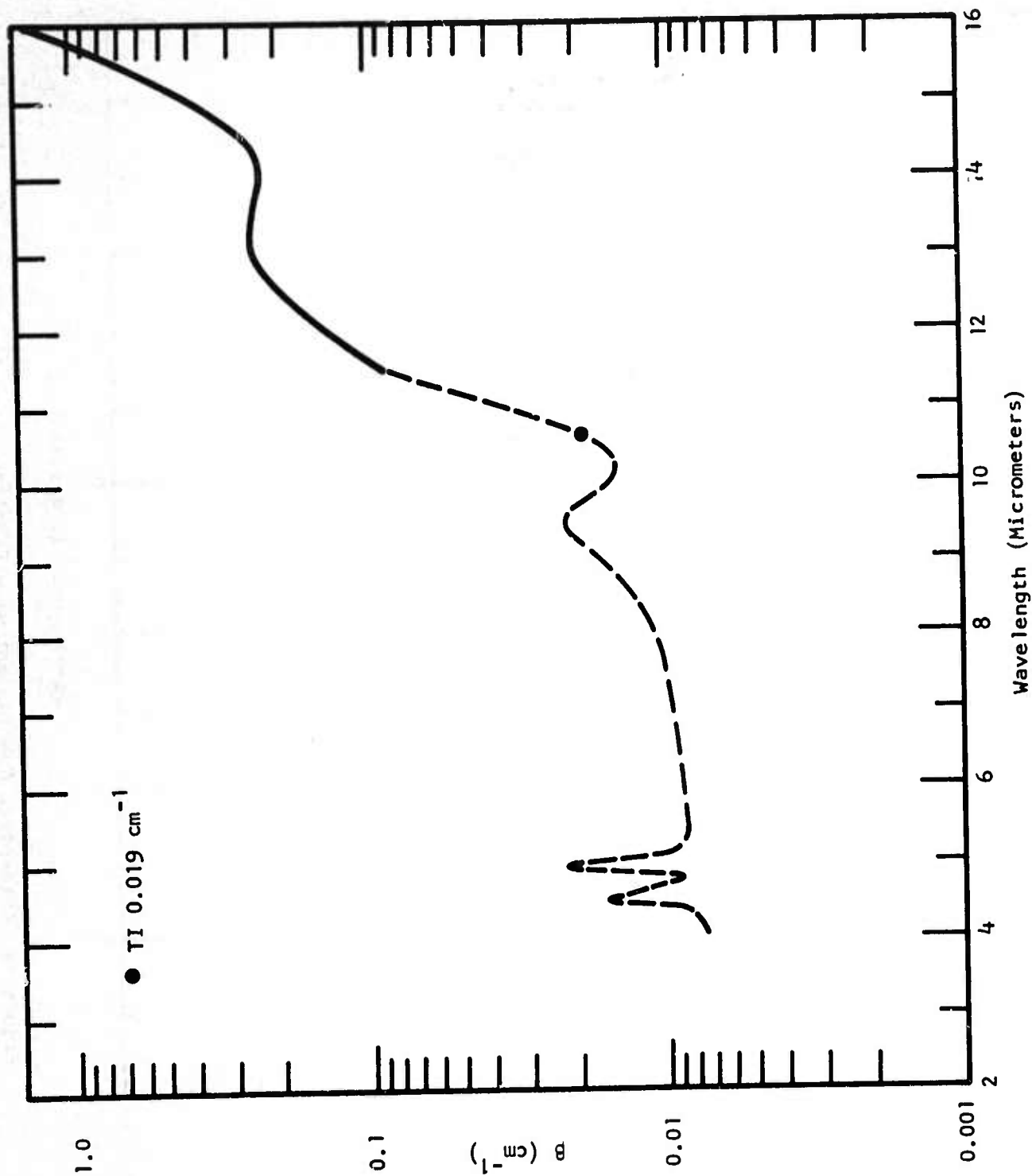
Figure 9 Absorption Coefficient as a Function of Wavelength for TI-1173-107
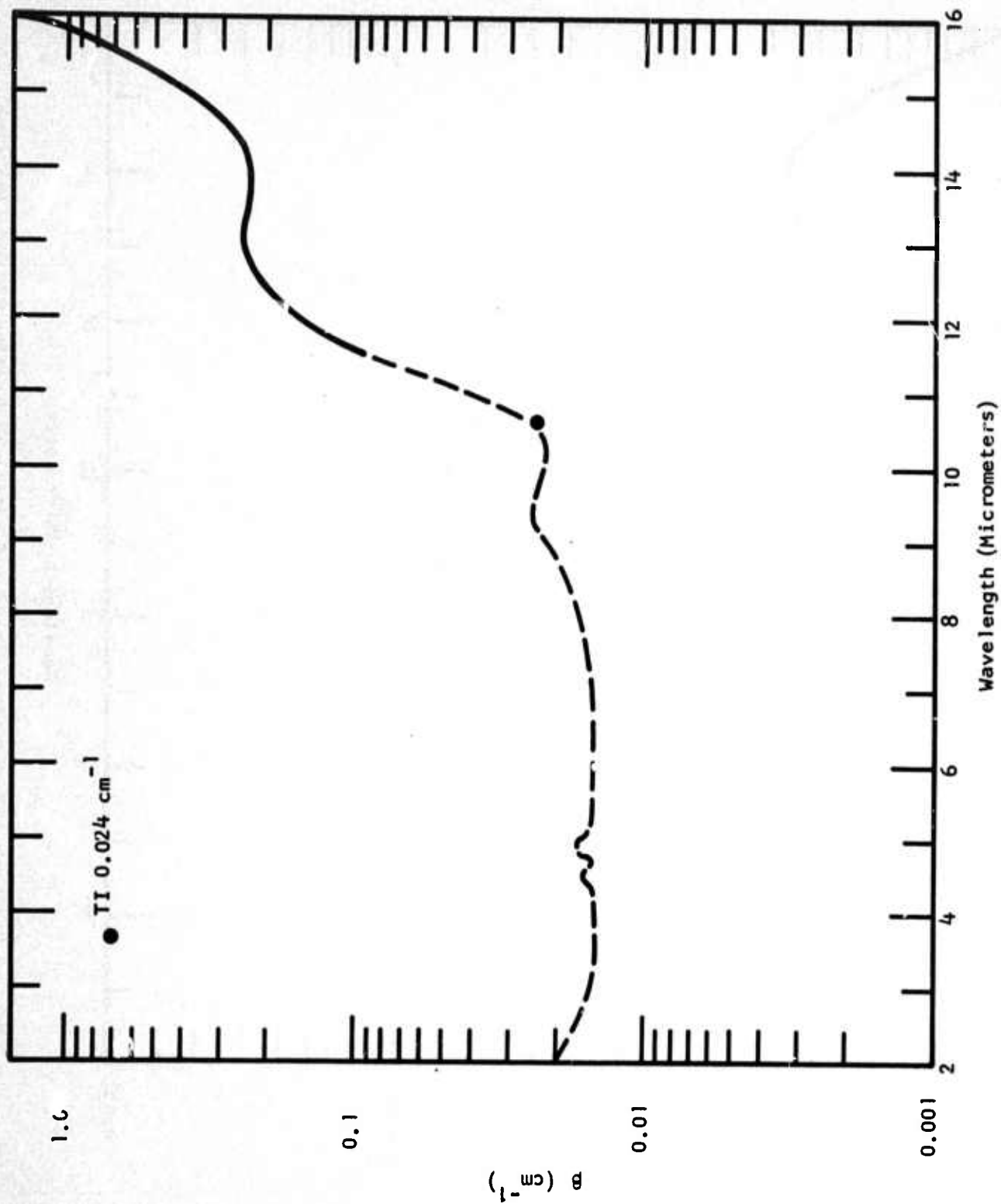
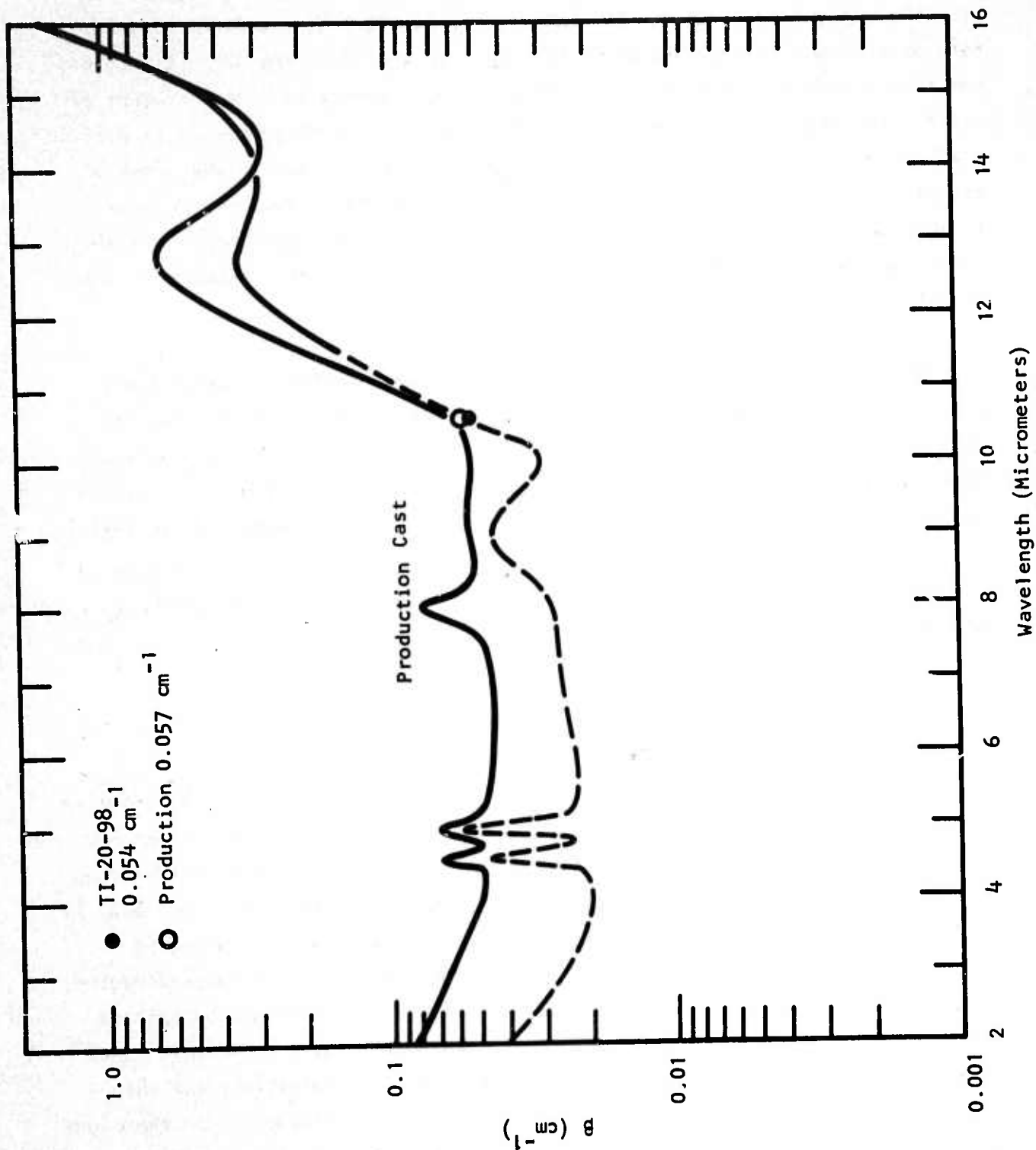Figure 10 Absorption Coefficient as a Function of Wavelength for TI-1173-109

28

Figure 11 Absorption Coefficient as a Function of Wavelength for TI-20-98

TI-20-98 and 0.057 cm^{-1} for production glass, have been added and agree well with the calculated results. The point to notice is that the magnitudes for both glasses are large relative to TI-1173. In addition, the production glass contains a peak around 8 µm which indicates the presence of a large amount of oxide. The magnitude of the 9.4 µm band is large for both glasses. In addition, examination of the glass using the infrared microscope revealed that some of the particulate matter was not filtered out by the frit. The arsenic seems to be a major contributor. Also, condensation from the vapors above the glass falls into the melt, leaving particles in the glass that are transparent, but visible in the infrared microscope.

The synthesis of another batch, TI-20-102, was carried out using three chambers (to separate the arsenic from the selenium), but no better results were obtained. The Ge-As-Se glasses appear much more difficult to synthesize than the Ge-Sb-Se glasses. Examination of past reports and notebooks reveals that the absorption level has been consistently higher in these glasses than in the Ge-Sb-Se glasses, with the absorption coefficient of the order of 0.05 cm^{-1} even in the 6 to 8 µm region. Work on TI-20 was discontinued, and efforts were concentrated on TI-1173.

C. Purity of the Glasses

1. Carbon

The as-received selenium residue left after distillation is amorphous carbon (according to x-ray analysis) in varying amounts. Measured carbon analyses have been in the 100 to 150 ppm range. Figure 12 illustrates the effectiveness of the distillation. On the left is an infrared microscope photograph (47X) of a TI-1173 witness sample prepared in the production area without selenium distillation. The glass was found to transmit 65.6% in the transparent region, thus passing the 65 to 67% transmission specification. It should be pointed out that the size and distribution of the carbon particles are variables that depend on reaction temperature, reaction time, physical agitation, and the beginning concentration of carbon in the selenium. The photograph on the right was taken using the same magnification of the laser calorimeter sample of TI-1173-102. Note that only one or two faint shadows of small particles are visible.

30
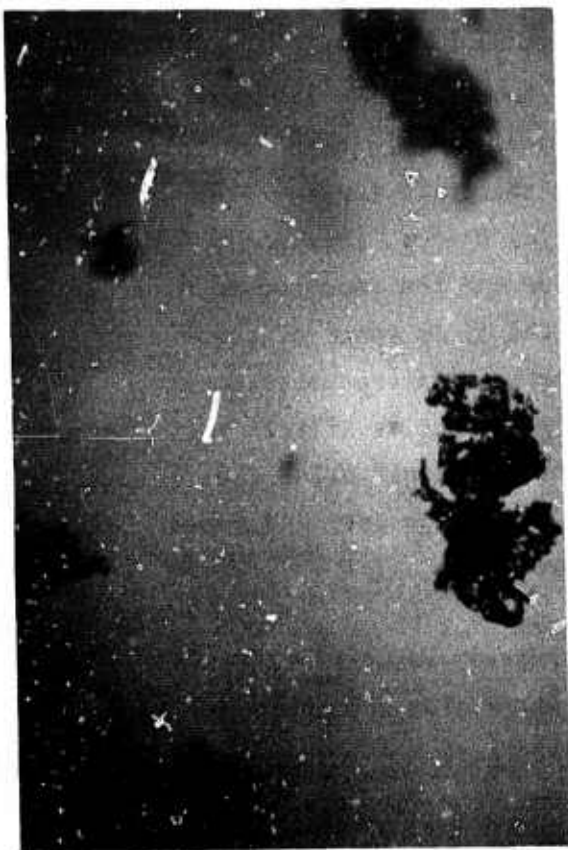
Production TI-1173
Glass (47X)

TI-1173-107 Laser Calorimeter
Sample (47X)

Figure 12   Infrared Microscope Images of Carbon Particles
in TI-1173

31

2. Emission Spectrographic Analysis

Results obtained from the analysis of TI-1173 and TI-20 samples prepared in this program consistently show the presence of Mg, Pb, Fe, and Cu in quantities from 0.1 to 1 ppm. These elements are commonly found as contaminants in semiconductor materials prepared at high temperatures in high purity quartz. As metallic impurities, the elements pose no threat to the infrared transmission of the glass. Even if they were present as oxides, they would pose no real problem because their concentration is low and the reported occurrence for their major absorptions is at wavelengths beyond the 15 μm range of concern. The only impurity we can identify that appears to be affecting transmission in the region of interest is Si. The silicon is probably present as silica and gets into the glass when the quartz containers are sealed off using the hydrogen torch. Table III presents a summary of the absorption data and important impurity results for the TI-1173 and TI-20 samples.

The [Si] and [Al] values are emission spectrograph results. The [O] values are the results obtained from the neutron activation procedure worked out at the Center for Trace Element Characterization at Texas A & M University.[3] The reliability figure placed on the results is ± 2 ppm. The absorption values listed are the laser calorimeter value for 10.6 μm, the peak in the absorption around 13 μm, obtained from IR transmission, and the absorption magnitude at around 9.4 μm obtained using our expanded-scale transmission measurement.

The first point to note is that no aluminum was deliberately added to the two production area glasses, TI-1173-P and TI-20-P; therefore, they had large absorptions at 10.6 μm and 13 μm. This fact is dramatically illustrated in Figure 13, which shows the measured transmission of TI-1173 about 1 cm thick with and without 5 ppm Al. The curve shows that the transmission at 10.6 μm is affected by the magnitude of the absorption at 12.8 μm. Almost identical curves have been reported in previous work at Texas Instruments[6] for TI-20 ($Ge_{33}As_{12}Se_{55}$) and for glass 56-8 ($Ge_{35}As_{15}Se_{50}$). The residual absorption that remains after addition of the Al is almost identical for all three glass compositions.

32

TABLE III

IMPURITIES AND ABSORPTION IN
TI-1173 AND TI-20 GLASS

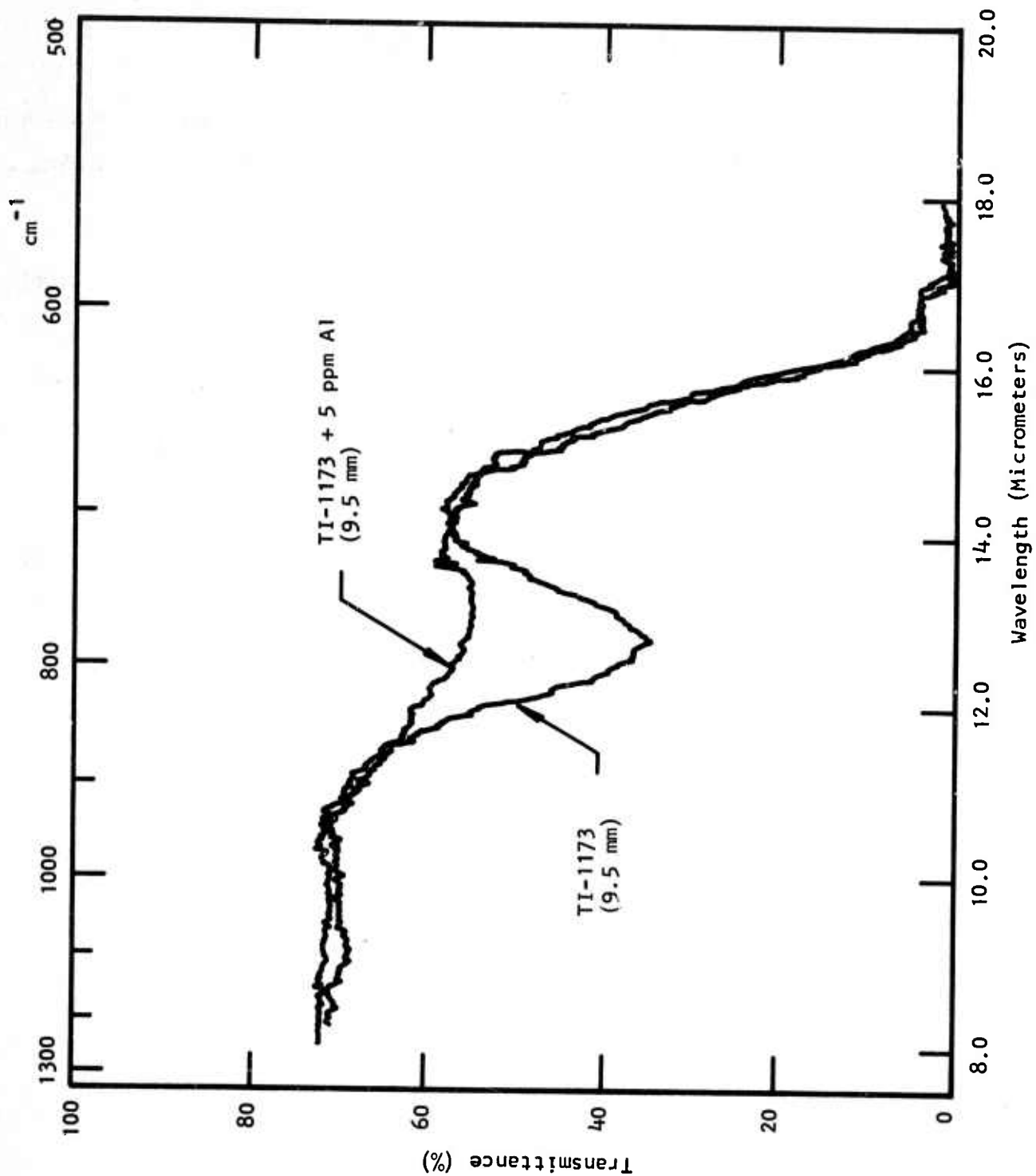| Glass	[Si] ppm	[O] ppm±2	[Al] ppm	β 10.6 μm cm^{-1}	$\beta \sim 13$ μm cm^{-1}	$\beta \sim 9.4$ μm cm^{-1}
1173-P	2.5	4	0.3[†]	0.06	0.65[†]	--
1173-92	1.4	5.5	6.1	0.012	0.19	0.0075
1173-107	2.6	5.5	6.3	0.019	0.25	0.022
1173-109	2.2	4.5	6.1	0.024	0.25	0.025
1173-122	1.1	--	5.7	0.013	0.22	0.015
20-P	2.2	6	0.4[†]	0.056	0.65[†]	--
20-98	4.4	5	5.3	0.053	0.34	0.045
20-102	3.3	-	5.6	--	--	--
Ge	N.D.	8	N.D.	--	--	--
Sb	N.D.	-	N.D.	--	--	--
Se	N.D.	-	N.D.	--	--	--

[†]No Aluminum Added

N.D. - Not Detected

Figure 13 The Effect of Trace Aluminum on the Infrared Transmission of TI-1173

34

Table III shows that the oxygen concentrations for the production glasses and the ones prepared in this program are essentially the same. TI-20 seems to have a little more oxygen than TI-1173, but otherwise the values (within experimental accuracy) are the same. The indicated [O] in germanium concentration is surprisingly high compared to our infrared value, for reasons unexplained at this time. One important factor is that the indicated oxygen concentration is almost identical to the aluminum concentration (5 ppm) found to be most effective in reducing the 12.8 μm absorption. This fact firmly supports the idea of the "gettering" action of the aluminum explaining why a larger quantity of trace metal provides no further reduction in absorption. In reality, two absorption bands must be present, one at about 12.6 μm due to the presence of oxygen (presumably Ge-O) and a second always present which is broad, low in magnitude, and centered about 13.4 μm in the Ge-Sb-Se glasses and about 12.8 μm in Ge-As·Se glasses.

D.   Discussion of Results for TI-1173 and TI-20

The only factor in Table III that shows any significant variation and correlation with the absorption in the glasses is the [Si] concentration. Note that Si was not detected in the reactants and probably gets into the glass during the sealing procedure. For this reason, our attempts to prepare glass with increased purity using the unbroken pieces of the low-oxygen germanium were thwarted by the increased exposure to silica brought about when the wide-mouth reaction chamber was sealed. To test this hypothesis, we synthesized another 1 kgm batch of TI-1173 using high purity reactants, hydrogen flow during oxide removal, and a reaction chamber designed to minimize the silica exposure of the ingredients during seal-off. The analytical results obtained are listed in Table III under run number 122. Notice the [Si] level is the lowest listed and that the laser calorimeter value is back in the 0.01 cm^{-1} range. The calculated absorption for TI-1173-122 is shown in Figure 14. Again, the laser calorimeter value at 10.6 μm has been added, and good agreement has been obtained with the curve estimated from scale expansion. Gas absorption in the 5 μm region is very high, indicating the dissolved H_2 was not removed during seal-off. The 9.4 μm absorption level is of the order of 0.015 cm^{-1}.
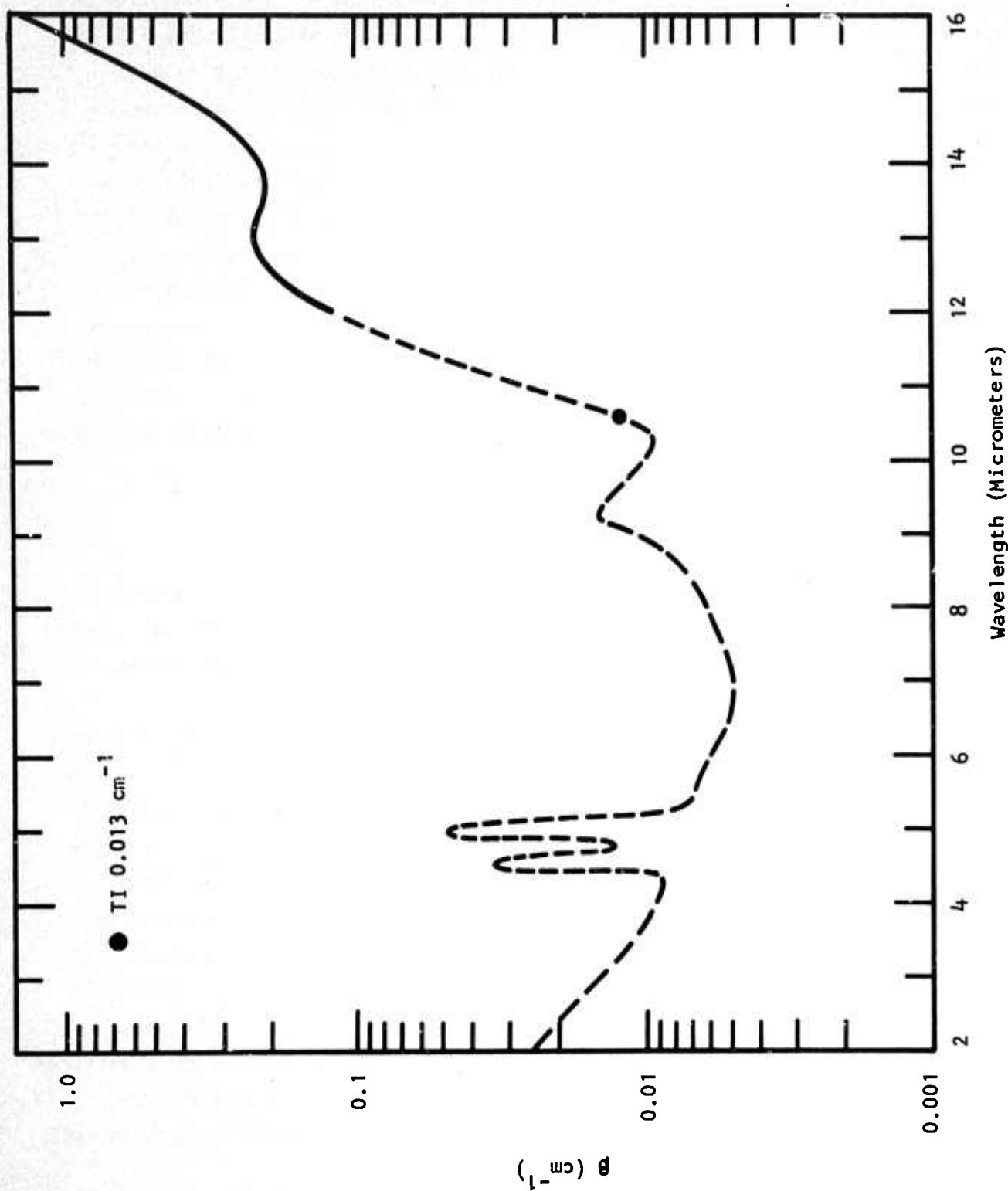
Figure 14 Absorption Coefficient as a Function of Wavelength
for TI-1173-122

A plot of the [Si] for the four TI-1173 samples as a function of the measured 10.6 μm absorption coefficient is shown in Figure 15. The only comparable value for TI-20 is shown as a (+) on the diagram. From all the information present, it appears that the absorption at 10.6 μm in TI-1173 at this degree of purity is dominated by the [Si], present probably in the form of silica. The absorption band at 9.4 μm occurs where the Si-O stretch generally is found. A better correlation between the 9.4 μm absorption and silicon content is shown in Figure 16. Again, the TI-20-98 value has been added, showing a direct correlation as well.

Examination of Figures 8 through 11 shows that the 9.4 μm absorption adds onto the absorption that occurs around 13 μm in both the Ge-Sb-Se and Ge-As-Se glasses. For the Ge-Sb-Se glass, the absorption center occurs at a wavelength slightly longer than 13 μm. Therefore, the domination of the 10.6 μm value is not as pronounced, and lowering the 9.4 μm level should lead to a lower 10.6 μm level. For the Ge-As-Se glass, the broad absorption is centered at a wavelength slightly less than 13 μm. The 10.6 μm value is dominated by that band more severely than the 9.4 μm band. Lowering the silica content will improve the 10.6 μm value only slightly.

E.   Origin of the Absorption at ∼ 13 μm in Ge-Sb-Se and Ge-As-Se Glasses

Lucovsky, et al.,[10] at Zerox and Mackenzie, et al.,[11] at UCLA have indicated that the IR absorption at 13.4 μm (744 cm^{-1}) in amorphous selenium is due to the presence of Se_8 rings. Mackenzie, et al.,[11] stated that the absorption could be made to disappear in a reaction catalyzed by the potassium ion. The Xerox work[10] showed that the band disappeared when arsenic was added to selenium, and a new band characteristic of As-Se appeared. Results obtained in our own laboratory[6] indicated that the 13.4 μm band did not disappear when germanium was added, but merely shifted to shorter wavelength (12.8 μm). Our results appeared to agree with and substantiate the Zerox conclusion[10] that in their experiments As was introduced into the Se_8 rings. For Ge-As-Se and Ge-Sb-Se glasses, the introduction of the elements into the ring shifted the frequency of the absorption and increased its magnitude. We speculated then that the effect of
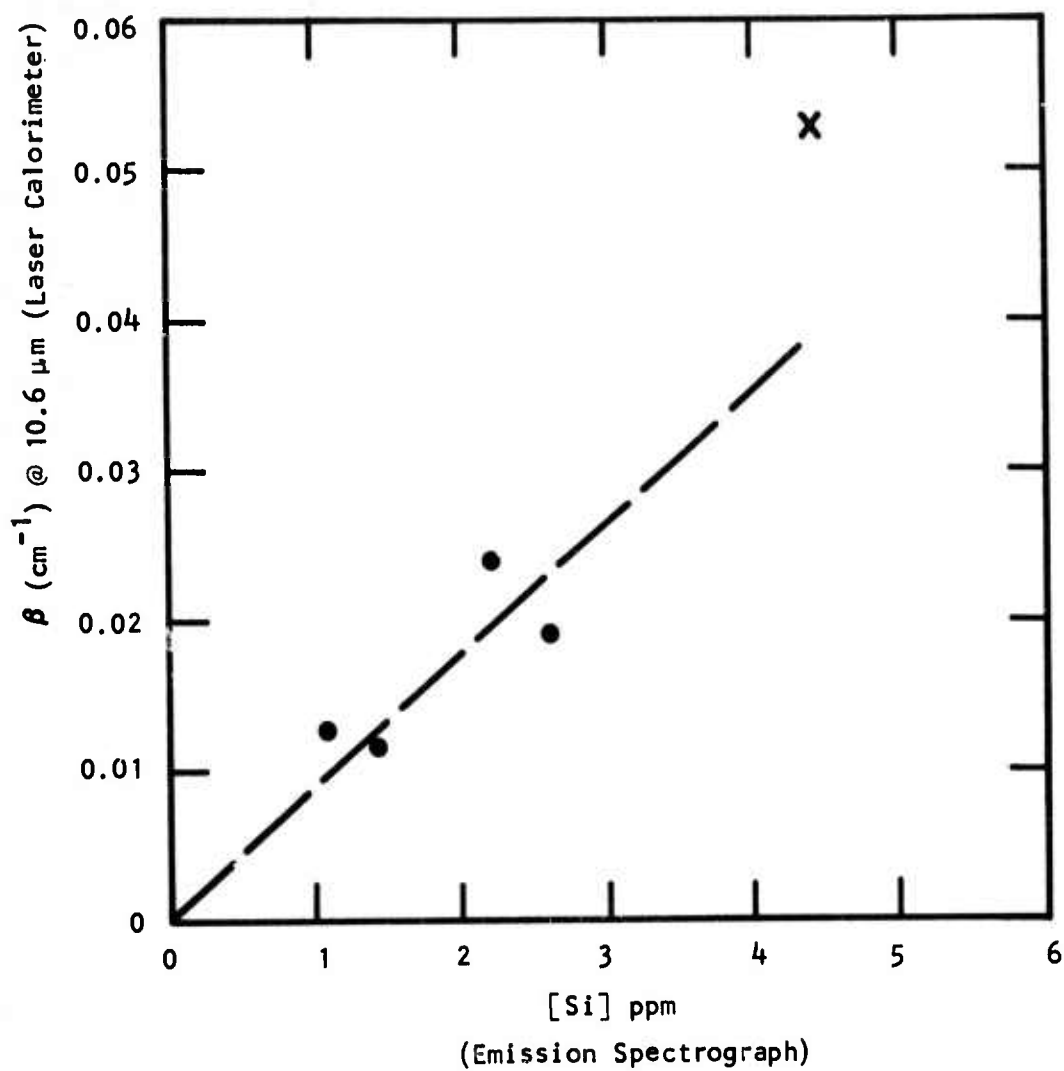
37

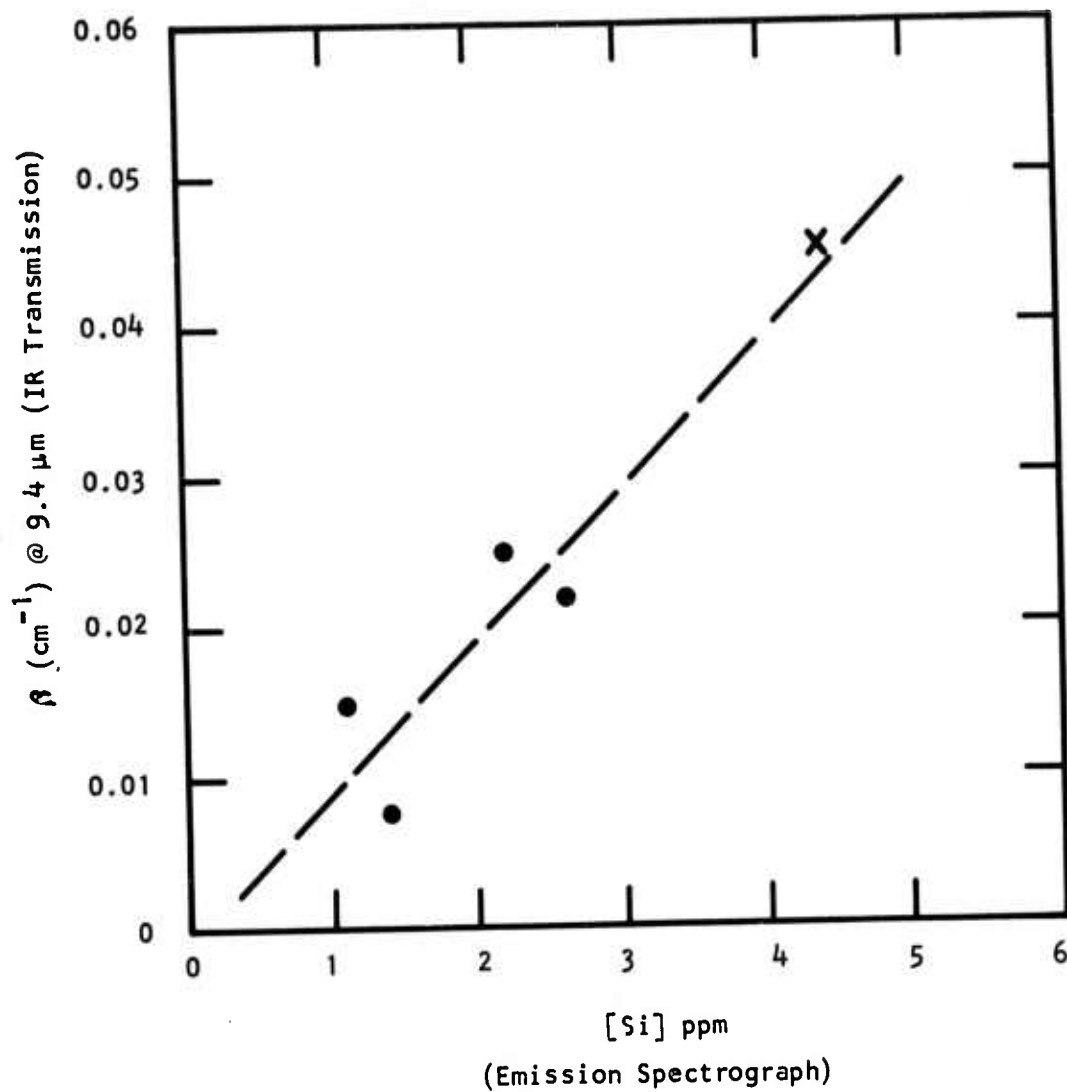Figure 15 Absorption at 10.6 μm in TI-1173 as a Function
of Silicon Content

Figure 16   Correlation Between Absorption at 9.4 μm and
Silicon Content

small amounts of Al, Zr, etc., was a catalyzed decomposition of the ring structure. However, in view of the results reported in the previous section, it appears the effect observed was due primarily to removal of the oxide absorption centered around 12.6 μm. In fact, when As or Ge was added to amorphous Se, the oxide that was introduced produced a band that far overshadowed the 13.4 μm band. Removing the effects of the oxide band leaves us with a band centered at almost the same frequency as the 13.4 μm band, a band considerably broadened and reduced in intensity from a magnitude of about 1 cm^{-1} to 0.2 cm^{-1}, a factor of five. If this band is related to the one found in pure amorphous Se, it is extremely difficult to explain how it could survive the dilution and reaction with 40 to 50 atom % of other elements.

The temperature dependence of the absorptions in the glasses is very important in helping to understand the origin of each. Absorptions arising from isolated impurities usually exhibit only weak temperature dependence, while intrinsic absorptions due to vibrational, electronic, or magnetic excitations generally show strong changes with temperature. To illustrate these statements, the transmittance of TI-1173 without the addition of Al and with the addition of Al measured between room temperature and 77 K is shown in Figures 17(a) and 17(b). The measurements were performed using the Perkin-Elmer E-1 system. Only small changes occur until a wavelength of 12.5 μm is reached for both glasses. This fact is illustrated by plotting the difference (77 K to room temperature) at the bottom of the curve showing the wavelength location of the thermally sensitive absorptions. In Figure 17(b), we find that the remaining absorption centered around 13.4 μm is reduced in magnitude and shifted toward shorter wavelength. The broad band in Figure 17(a) shifts to 12.7 μm, indicating the impurity band is centered more nearly at 12.6 μm. Combining the two bands still leads to a peak at 12.8 μm. Prior to the successful preparation of high purity gettered TI-1173 glass, the strong oxide absorption at 12.6 μm obscured the thermally active absorption in this spectral region. To learn more about the thermally active character of this band, the measurements were extended to higher temperatures over the wavelength range out to 18 μm. The results covering -196°C to +207°C are shown in Figure 18. The temperature dependence is quite strong, particularly for temperatures in excess of ambient. Assuming the absorption peak varies in a power law manner, $\alpha \sim T^x$, the absorption coefficient
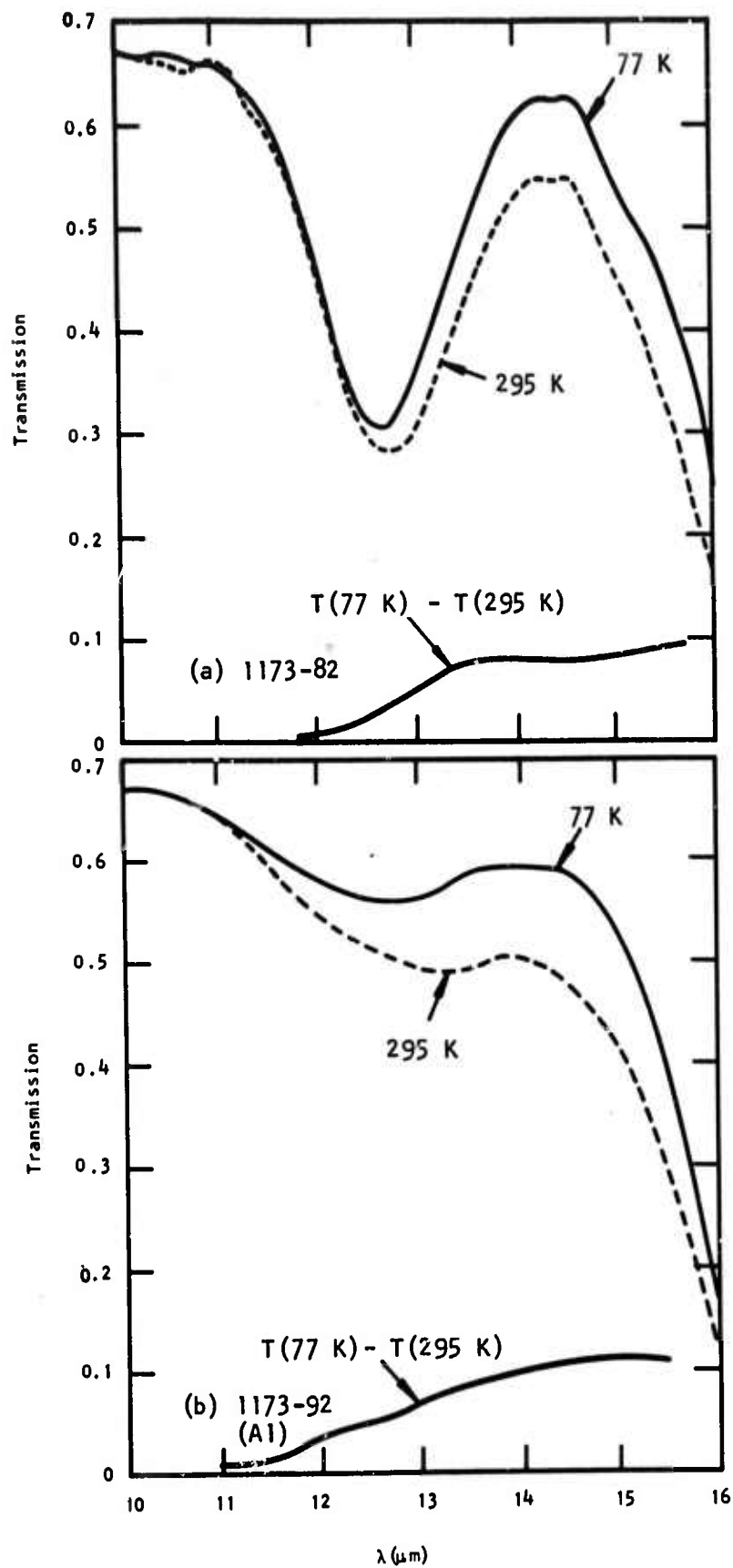
40

Figure 17 Transmission of TI-1173 With and Without Aluminum as a Function of Temperature
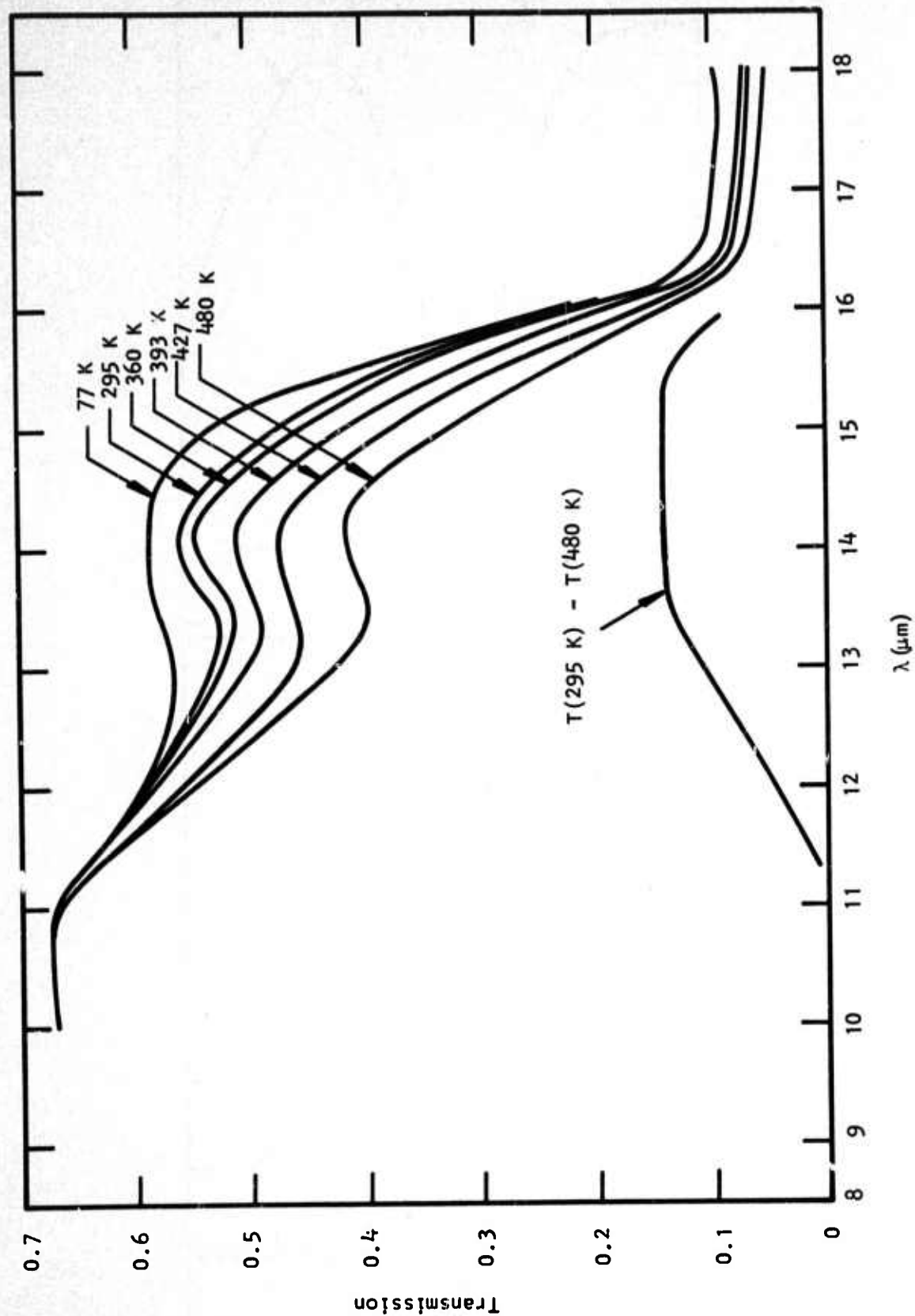
Figure 18 Transmission Above and Below Room Temperature of TI-1173 Treated with Trace Aluminum

at 13 μm was found to have the value of $x = 1.85 \pm 0.15$, within the predicted temperature dependence for a third order multiphonon excitation. However, there is some discrepency in the wavelength location of the peaks. From IR reflection spectra obtained in our laboratory, the strongest absorption is estimated to occur at 235 cm^{-1}, with an absorption maxima estimated to be 7500 cm^{-1}. A confirmation of the resonance frequency is found in the Raman data reported to us by Dr. Marvin Hass of NRL. Dr. Hass reported two frequencies for $Ge_{28}Sb_{12}Se_{60}$: 230 cm^{-1} and 193 cm^{-1}. Doubling and tripling our 235 cm^{-1} value leads to 470 cm^{-1} and 705 cm^{-1}, in contrast to the observed values of 490 cm^{-1}, 560 cm^{-1}, and 745 cm^{-1}. A $\omega/\omega f$ plot for TI-1173 is shown in Figure 19 for room temperature and liquid nitrogen data. The slopes for an exponential decay from the $\beta_o = 7500$ cm^{-1} of $\beta \sim \beta_o e^{-2\omega/\omega f}$ and $\beta \sim \beta_o e^{-3\omega/\omega f}$ are shown as dashed lines for reference. Note that the dependence for the peaks in absorption, below room temperature, is slight.

The final illustration for TI-1173 describes the present condition of the absorption at the band edge. Results obtained in our laboratory are shown in Figure 20. The work of Tauc and Menth[12] has been added for reference. Their values are found to be more than one order of magnitude above our own. However, we know nothing of the quality of the $Ge_{28}Sb_{12}Se_{60}$ glass on which their measurements are based. The lowest curve represents the results obtained in another program in our laboratory[13] and is based on near-IR laser calorimeter values. The upper curve was obtained strictly from transmission measurements using a conventional spectrophotometer. The exponential absorption edge extrapolation to 10.6 μm indicates the level of absorption is not presently limited by the fundamental electronic absorption process.

F.   Other Experiments

The possibility of surface contamination or surface oxides contributing to the absorptions was also considered. The two end surfaces of a cylindrical TI-1173-92 sample were subjected to Ar ion milling with about 1 μm of material removed over a 1 cm diameter area. Infrared transmittance measurements were carried out from 2 to 18 μm on the 7X scale of the Perkin-Elmer 221. Direct
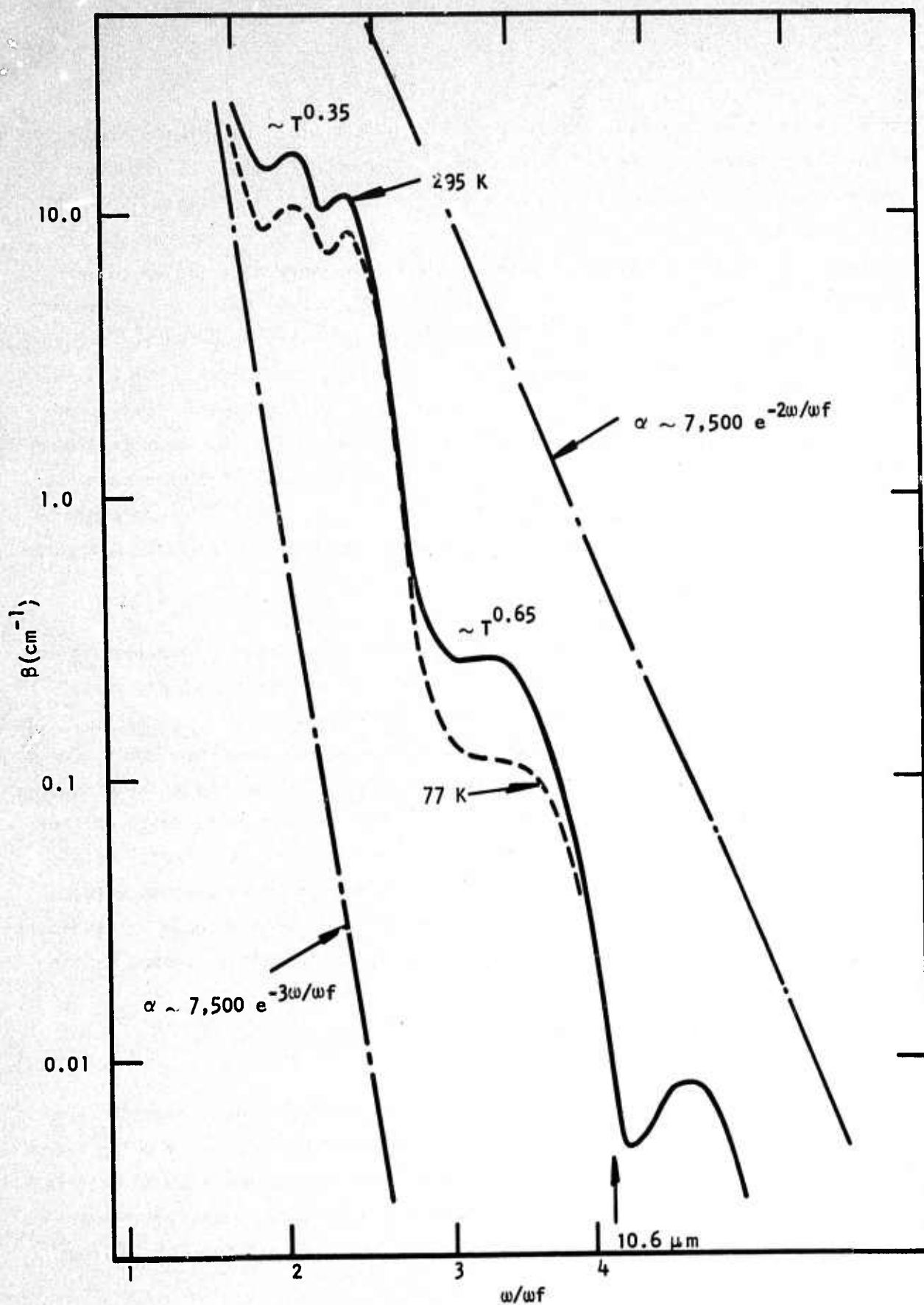
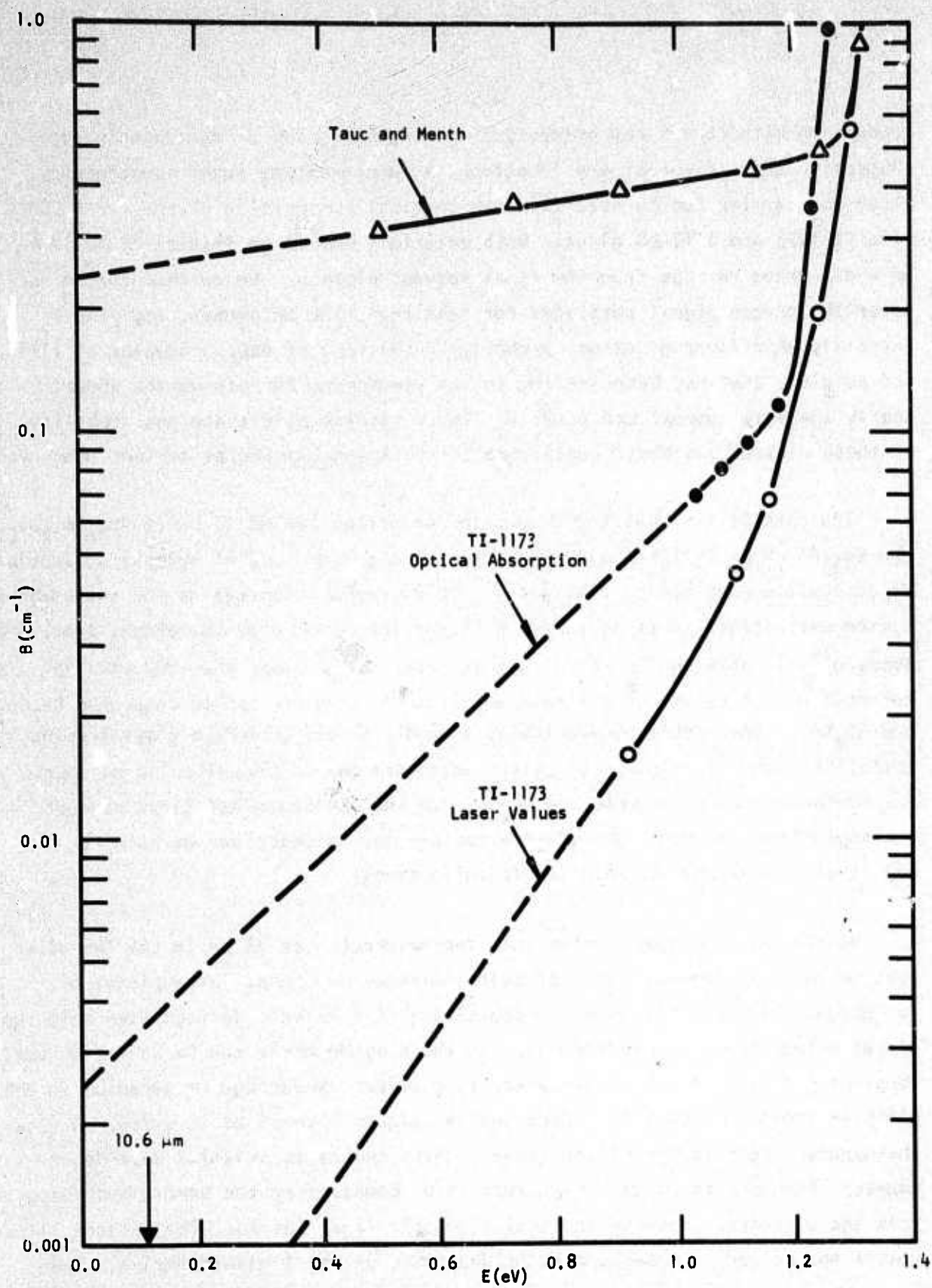Figure 19 Plot of Absorption as a Function of ω/ωf for TI-1173 at 77 K and 295 K

44

Figure 20 The Absorption Edge of TI-1173

comparison with curves run before ion milling indicated no decrease in the absorption coefficient at any location. A supplementary Auger spectroscopy study was carried out to ascertain the chemical composition of the first 500 Å of a TI-1173 and a TI-20 glass. Both materials showed an initial 20 to 30 Å of hydrocarbon residue from the final solvent cleanup. Below this contamination layer the oxygen signal persisted for less than 10 Å thickness, implying an extremely thin layer of oxide, probably in the form of GeO_2. Samples of 1173 and 20 glass that had been sitting in the atmosphere for six months showed nearly the same composition profile. These results illustrate the stability of these glasses and their resistance to surface oxidation at ambient temperatures.

The possibility that the absorption occurring around 13 μm in $Ge_{28}Sb_{12}Se_{60}$ and $Ge_{33}As_{12}Se_{55}$ is intrinsic suggests that the magnitude of absorption should be composition-dependent. The glass-forming composition region for the Ge-Sb-Se system established in earlier work at Texas Instruments by Patterson, Brau, and Johnson[14] is shown in Figure 21. It is important to note that the TI-1173 composition point lies on a line drawn from the stoichiometric compounds Ge_2Se_3 and Sb_2Se_3. The region toward the pure chalcogen represents a glass-forming composition region in which the glass structure may be described as polymeric and containing selenium-selenium bonds. On the chalcogen-deficient side of the stoichiometric line, the glass structure may be described as network and likely to contain no selenium-selenium bonds.

On the basis of the premise that the absorption at 13 μm in the two glass systems reflects the existence of selenium-selenium bonds, large pieces of low oxygen, high purity, aluminum-containing TI-1173 were diluted with selenium, representing then a composition line in the diagram where the Ge/Sb ratio remained constant. A plot of calculated absorption versus percentage of selenium in the glass is shown in Figure 22. Each sample weighed a total of 50 grams. Notice the apparent correlation of the curves, which indicates selenium dependence. However, attempts to repeat these results by compounding the same glass composition from the elements, crossing the stoichiometric line, failed. The failure illustrates the danger in drawing conclusions based on small glass samples. The
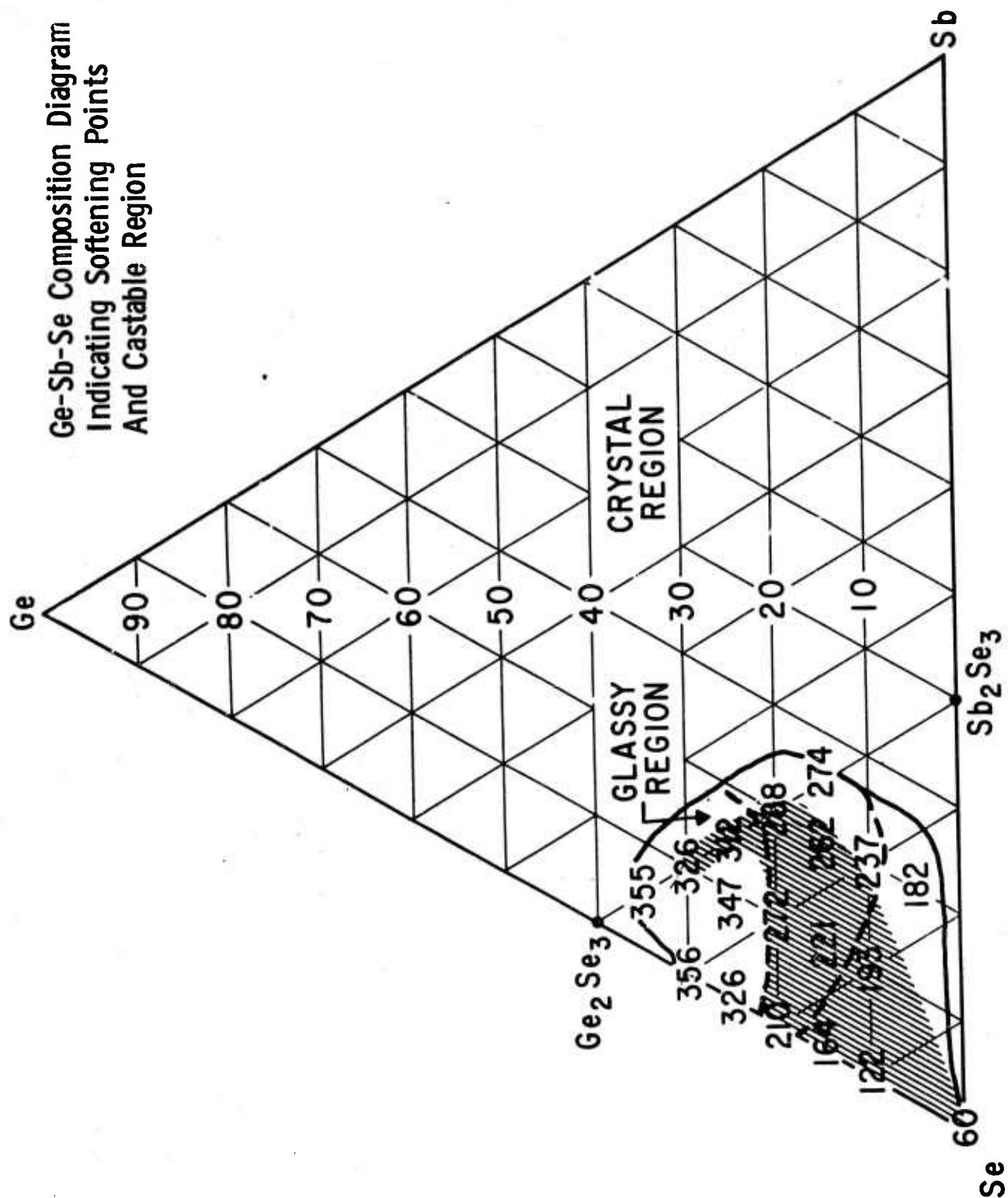
Ge-Sb-Se Composition Diagram
Indicating Softening Points
And Castable Region

Figure 21 Glass-Forming Composition Region for the Ge-Sb-Se System
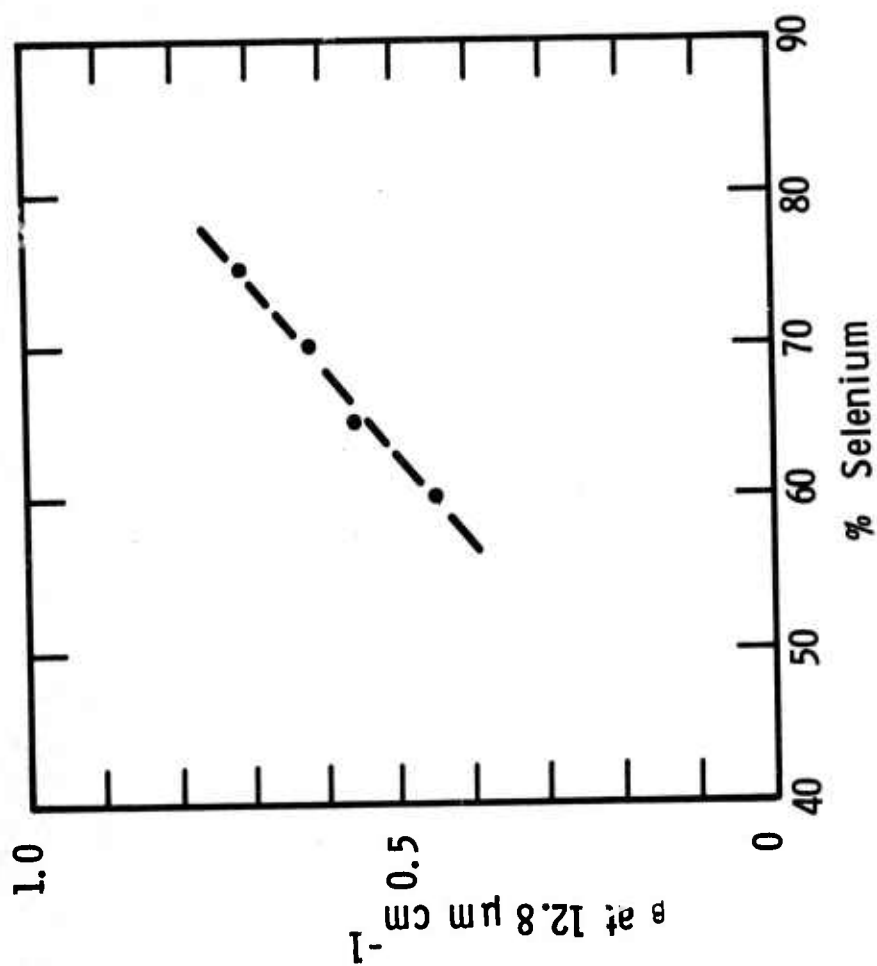
47

Figure 22 Absorption at 12.8 μm for TI-1173 Diluted with Selenium

apparently excellent correlation reflected the amount of oxide-containing selenium added to the oxide-free TI-1173 to produce the desired composition. Contamination, which is always a problem, is an especially great problem when one is working with small quantities of glass. In all, five different sets of glass compositions covering the glass-forming region around TI-1173 on both sides of the stoichiometry lines were prepared. Some were in quantities of 100 gm or more. No relationship with composition was established, nor was the absorption appreciably changed.

Large amounts of Al were found to produce no further change in absorption than did the 5 to 10 ppm quantities. Amounts up to 1000 ppm, even 1 to 2 atom %, were used. The larger quantities promoted an attack on the quartz container, as indicated by the appearance of "silicate" bands. Trace quantities of silver, magnesium, and potassium chloride were used with no apparent effect. However, zirconium and copper were found to be effective. Large amounts of copper (1 to 2 atom %) were used in the belief that a planar, four-coordinated structure might be generated that would be different from that of germanium. However, the transmission again had the same appearance one would obtain with 5 to 10 ppm Al. Most probably, the "oxide gettering" explanation will prove out; however, there are some discrepancies if the gettering action effectiveness is based on free energy of formation of the oxides. The failure of magnesium to function is the most obvious failure.

Attempts to prepare "silica"-free glass in a non-quartz container have been unsuccessful so far. One attempt, using a graphite chamber sealed in a quartz tube and maintained in a vertical position, failed because the high-density Poco Graphite was permeable to the melt. Attempts to use boron nitride containers in a similar manner have failed due to oxide contamination. Future attempts will be based on minimizing the quantity of silica released during seal-off.

SECTION V

INTERDEPENDENCE OF PHYSICAL PARAMETERS

A. Density

Published results from this laboratory[15] for selenium-based and tellurium-based glasses demonstrated a linear relationship between the calculated molecular weight for a glass composition and its density. At the time, very little data was available for sulfur-based glasses. The data available for As_2S_3 and S indicated that sulfur-based materials would lie on a line of slope different from that of selenium- or tellurium-based glasses. During the present program, several sulfur-based glasses were made available to us by workers on another glass program.[16] Addition of these points confirm the earlier speculation. Figure 23 shows a plot of measured density as a function of molecular weight for sulfur- and selenium-based glasses. Two separate slopes are obtained, with a mixed S-Se glass in between.

B. Thermal Expansion and T_g

A review article by Gschneider[17] pointed out that for over 85 years investigators have noted that crystalline materials with high melting points have low coefficients of thermal expansion, and vice versa. Sakka and Mackenzie[18] pointed out recently that a simple empirical rule,

$$T_g/T_m = 2/3 \quad ,$$

where T_g is the glass transition temperature and T_m is the crystalline melting point, holds suprisingly well for inorganic systems. Putting these two observations together, one would expect glasses with high T_g to have low coefficients of expansion. The measured values for many glass compositions are shown in Figure 24. The general trend is apparent, but there is considerable variation among glasses of widely different composition. Since T_g should reflect the weaker, long-range forces in a multicomponent system, it should not be surprising to see some compositions vary widely from expected behavior. For example, the
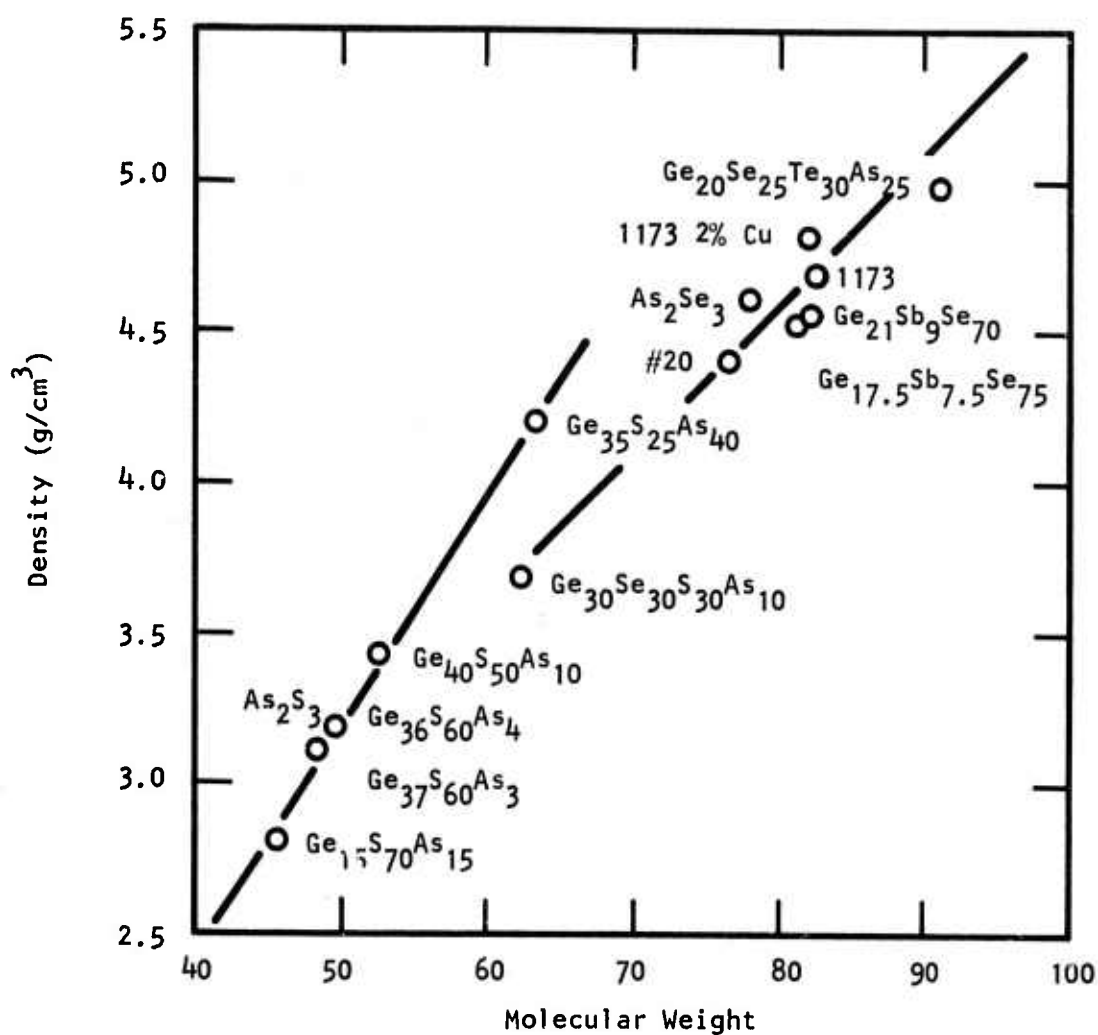
50

Figure 23 Density as a Function of Molecular Weight for Some
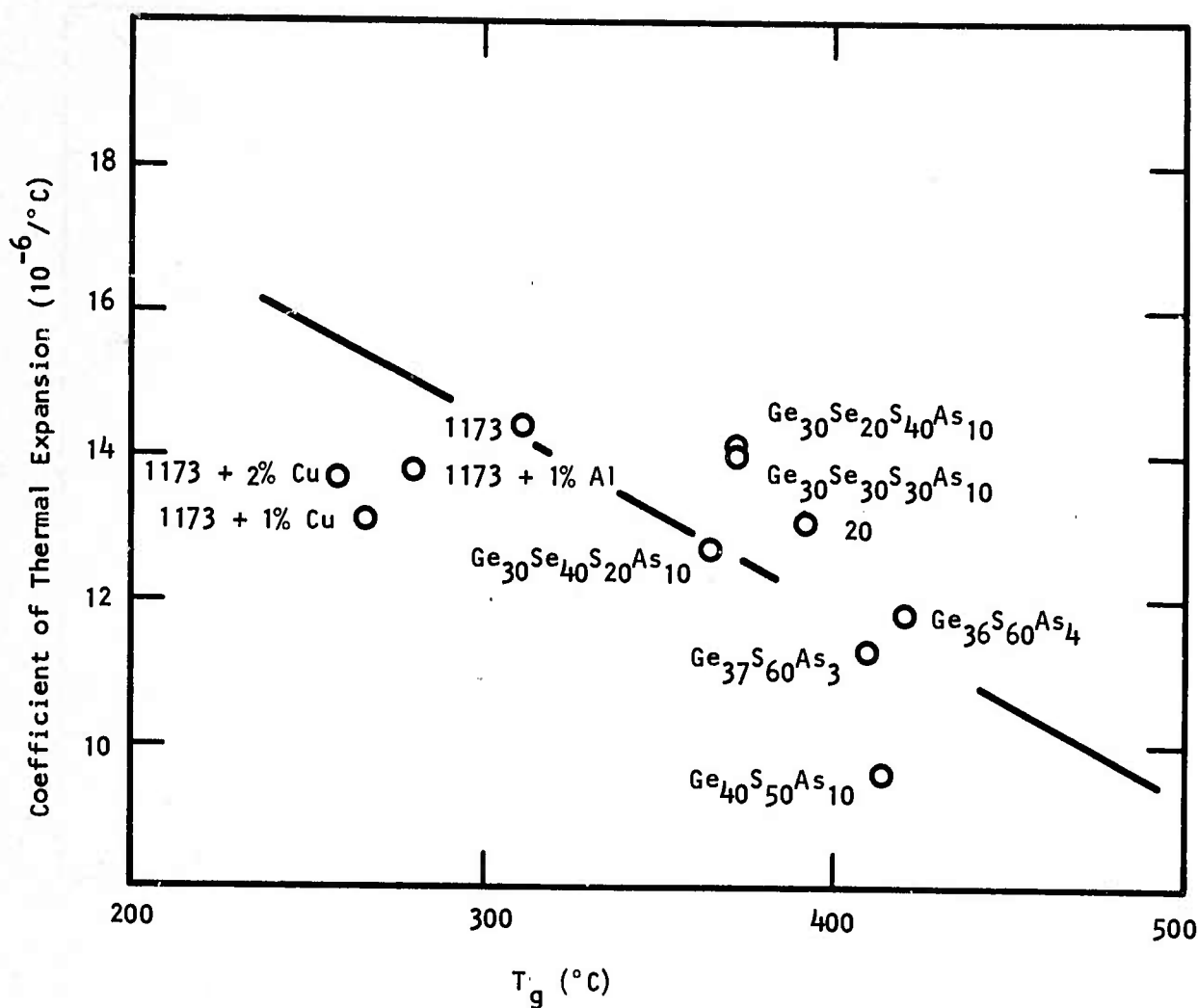Selenium and Sulfur Glasses

Figure 24 Thermal Coefficient of Expansion and Glass Transition
Temperatures (T_g) for Some Sulfur and Selenium Glasses

points for 1%, 2% Cu in TI-1173 and the point for 1% Al in TI-1173 show both T_g and the volume expansion decreasing from the values for pure TI-1173. With a decrease in volume expansion, one would expect T_g to increase. An explanation for this apparent discrepancy is that the addition of Cu or Al leads to the formation of small molecules which fit into the void spaces in the network structure. Thus, the long-range forces between the network units are weakened.

C. Elastic Moduli

Table IV lists the Young's modulus and the shear modulus as determined from sound velocity measurements for several glass compositions. The calculated Poisson's ratio for each composition is given in the third column. A second value for TI-20 taken from the literature[19] is shown for comparison to indicate the accuracy and reproducibility of the method.

Note the decrease in Poisson's ratio as composition is changed from glassy selenium toward the network structure glass TI-1173. The value decreases, indicating a change from polymeric to network form. The other two glasses listed in the series have the same Ge/Sb ratio as $Ge_{28}Sb_{12}Se_{60}$, TI-1173. Even lower values of Poisson's ratio are noted for sulfur-based glasses that are high in Ge and As, but low in sulfur. Increases in elastic moduli of 2 to 4 times the selenium value are found for sulfur-based materials.

D. Hardness

A straight-line relationship between the measured hardness and Young's modulus is found for the selenium-based and sulfur-based glasses shown in Figure 25. The slopes for the two families of glasses are different, reflecting the relative strengths of the primary bonds.

E. Thermal Conductivity

1. Composition Dependence

The room temperature values of thermal conductivity for 14 chalcogenide glasses of different compositions were obtained using the Thermal Comparator.

TABLE IV

ELASTIC MODULI OF SULFUR- AND SELENIUM-BASED GLASSES

|	E (10^6 psi)	G (10^6 psi)	ν
Se	1.43	0.545	0.315
$Ge_{17.5}Sb_{7.5}Se_{75}$	2.35	0.92	0.279
$Ge_{21}Sb_9Se_{70}$	2.56	1.00	0.278
$Ge_{28}Sb_{12}Se_{60}$ (1173)	3.11	1.22	0.268
As_2Se_3	2.65	1.03	0.289
#20	3.17	1.26	0.266
#20 (Bell Labs[19])	3.29	1.31	0.261
$Ge_{15}S_{70}As_{15}$	2.01	0.776	0.295
$Ge_{36}S_{60}As_4$	3.05	1.22	0.250
$Ge_{37}S_{60}As_3$	3.37	1.38	0.244
$Ge_{40}S_{50}As_{10}$	4.26	1.70	0.251
$Ge_{35}S_{25}As_{40}$	6.08	2.39	0.271
$Ge_{30}Se_{30}S_{30}As_{10}$	2.72	1.02	0.274
$Ge_{20}Se_{25}Te_{30}As_{25}$	3.00	1.18	0.270
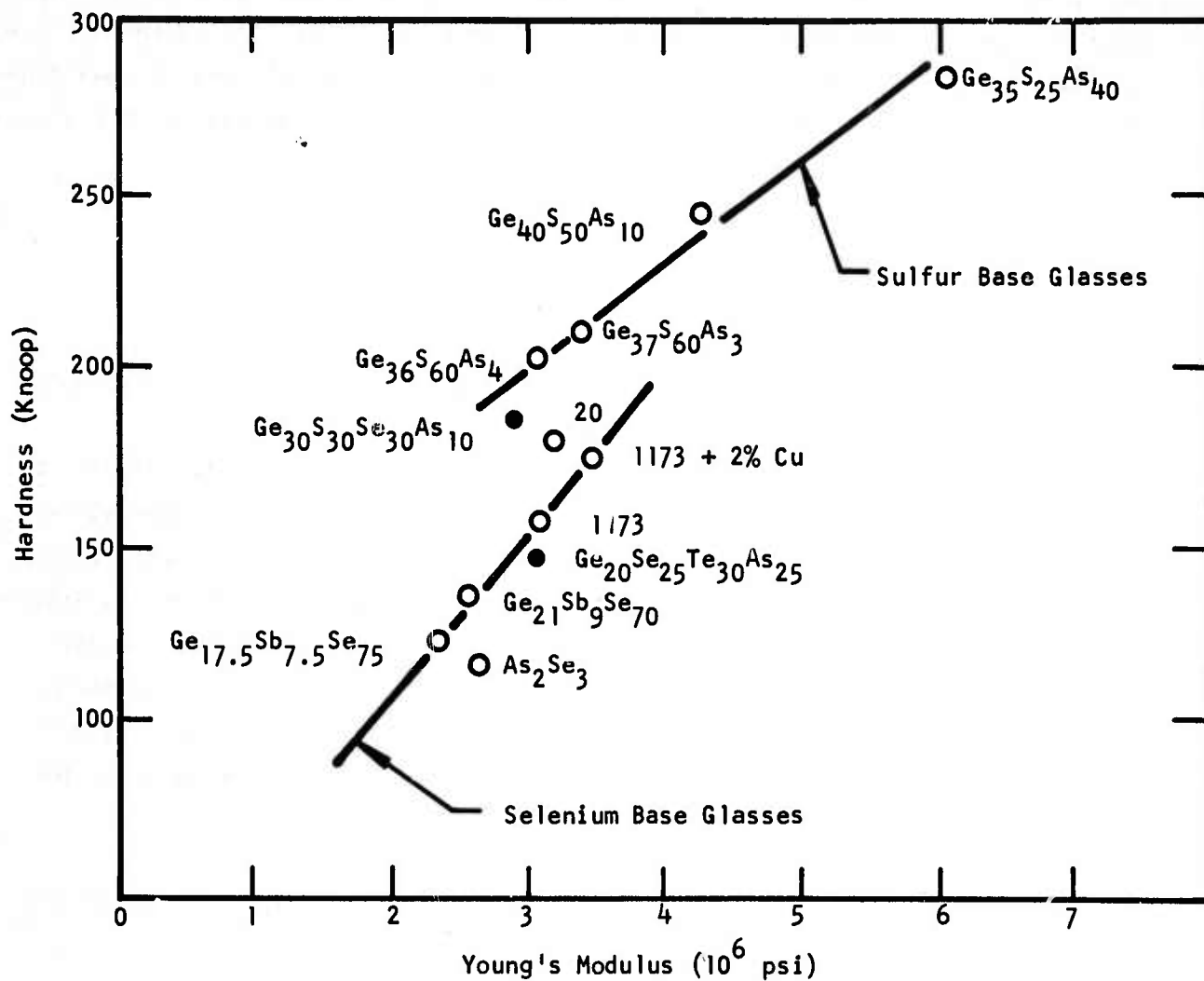
Figure 25   Hardness vs Young's Modulus for Sulfur and Selenium Glasses

These values are plotted as a function of their respective longitudinal sound velocities (also measured at room temperature) in Figure 26. An excellent linear correlation is observed.

Štouraĉ, et al.,[20] reported in 1968 the measured thermal conductivities for a series of Ge-Se glasses. The observed increase in thermal conductivity with increasing germanium content was explained as being related to the observed increase in sound velocity. The results of Štouraĉ, et al.,[20] and our own linear relationship may be explained by applying the simple Debye expression for thermal conductivity due to phonons:

$$K = \tfrac{1}{3} C_v \, V \, \overline{l} \quad ,$$

where C_v is the heat capacity per unit volume,

$\quad$ V is the average phonon velocity (related to the sound velocity), and

$\quad$ $\overline{l}$ is the mean free path for phonons.

Workers at Catholic University pointed out[21] that the heat capacity values for TI-1173 and TI-20 reach almost their maximum values (3R) by room temperature. For chalcogenide glasses with low Debye temperatures C_v would be expected to vary only slightly with composition. The value of $\overline{l}$ is a measure of the disorder (or lack of three-dimensional order) for the melt-formed glasses and should change very little with composition. The only remaining function, the sound velocity, must change with composition and as it changes, affect the thermal conductivity. The linear relationship will be most helpful in predicting the thermal conductivity of new glass compositions.

Examining the absolute values of thermal conductivity for TI-1173, TI-20, As_2Se_3, etc., we find values orders of magnitude below those of crystalline materials. For application with high energy lasers, these low thermal conductivity magnitudes are perhaps the most serious disadvantage of glass materials. Examining the values for sulfur glass composition we can see that an order of magnitude improvement is not a possibility.
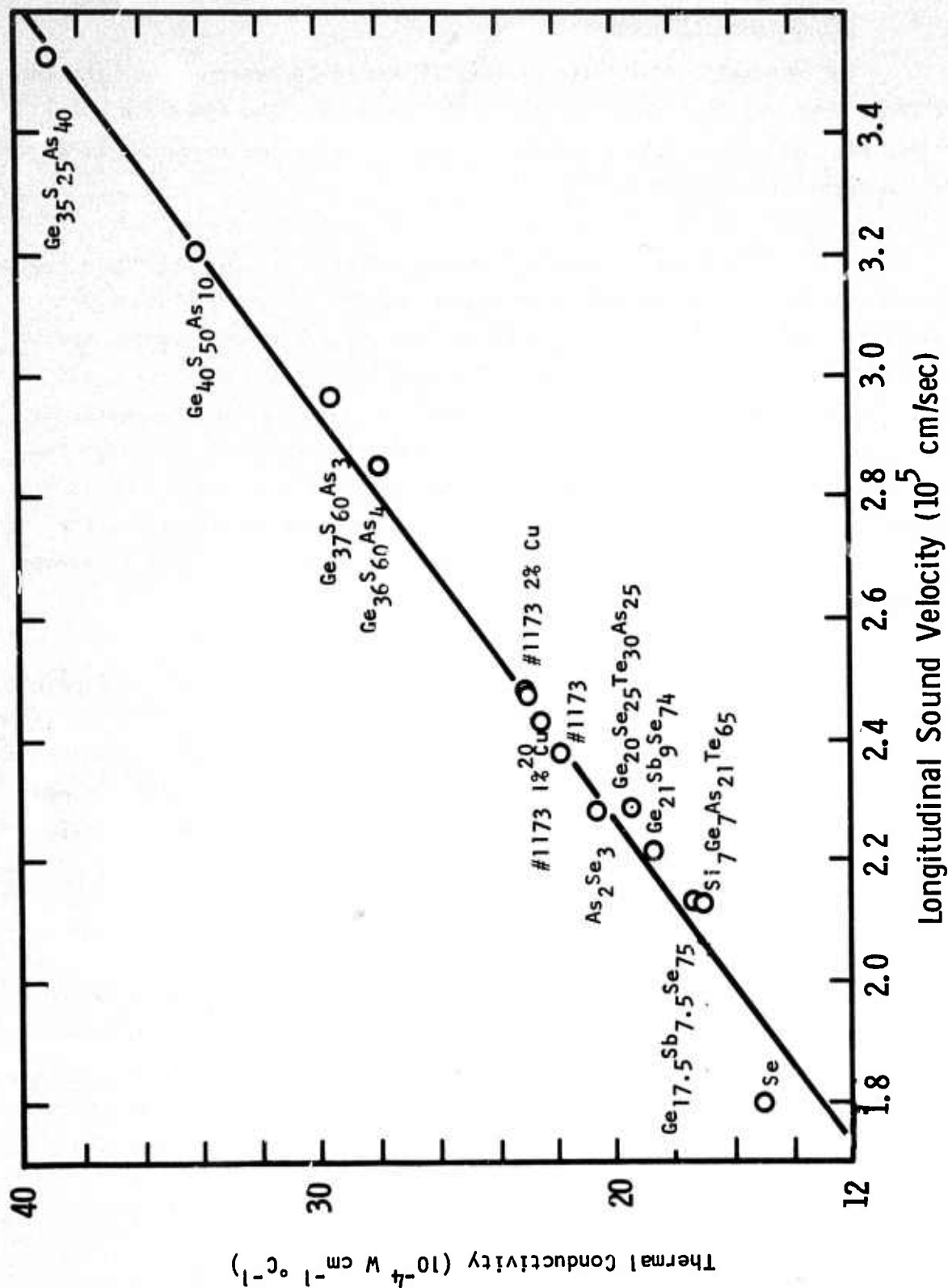
Figure 26 Thermal Conductivity vs Longitudinal Sound Velocity for Some Sulfur and Selenium Glasses

2. Temperature Dependence

The thermal conductivity of TI-1173 and TI-20 measured over the temperature range from -60°C to +200°C is shown in Figure 27. The plots are quite similar, with an almost linear temperature dependence. The values of TI-20 are about 5% higher than those for TI-1173.

Both glasses are transparent to the infrared in the wavelength region in which the peak of energy emitted from blackbodies (or gray) above room temperature should occur. For that reason, part of the energy transmitted by the solid is energy emitted from the hot surface in contact with the glass plate. To gain some estimate of the magnitude of this portion, the surfaces of the glass plate were coated with a low emissivity, opaque gold film. The remeasured values are shown in the lower dashed line for TI-1173. The correction is appreciable, especially at the higher temperatures, and brings the measured absolute value using the temperature apparatus almost into agreement with the Thermal Comparator value.

The observed increase in thermal conductivity with increasing temperature is in contrast to what is generally observed with crystalline solids except at very low temperatures. In the normal range, the change in value with temperature is found to follow the slight change in heat capacity.[22] Referring again to the Debye thermal conductivity expression, our laboratory results indicate very slight decrease in sound velocity with increasing temperature.

F. Rupture Modulus of TI-1173

The rupture modulus was measured on 12 samples of TI-1173 in three-point loading with bottom supports 2.0 inches apart. The dimensions of the samples were 2.50 x 0.620 x 0.342 inches. The loading rate was 0.02 inch per minute. The average rupture modulus for the twelve samples was 3028 psi with a standard deviation of 384 psi. The rupture moduli are given in Table V along with the location of the fracture origin.
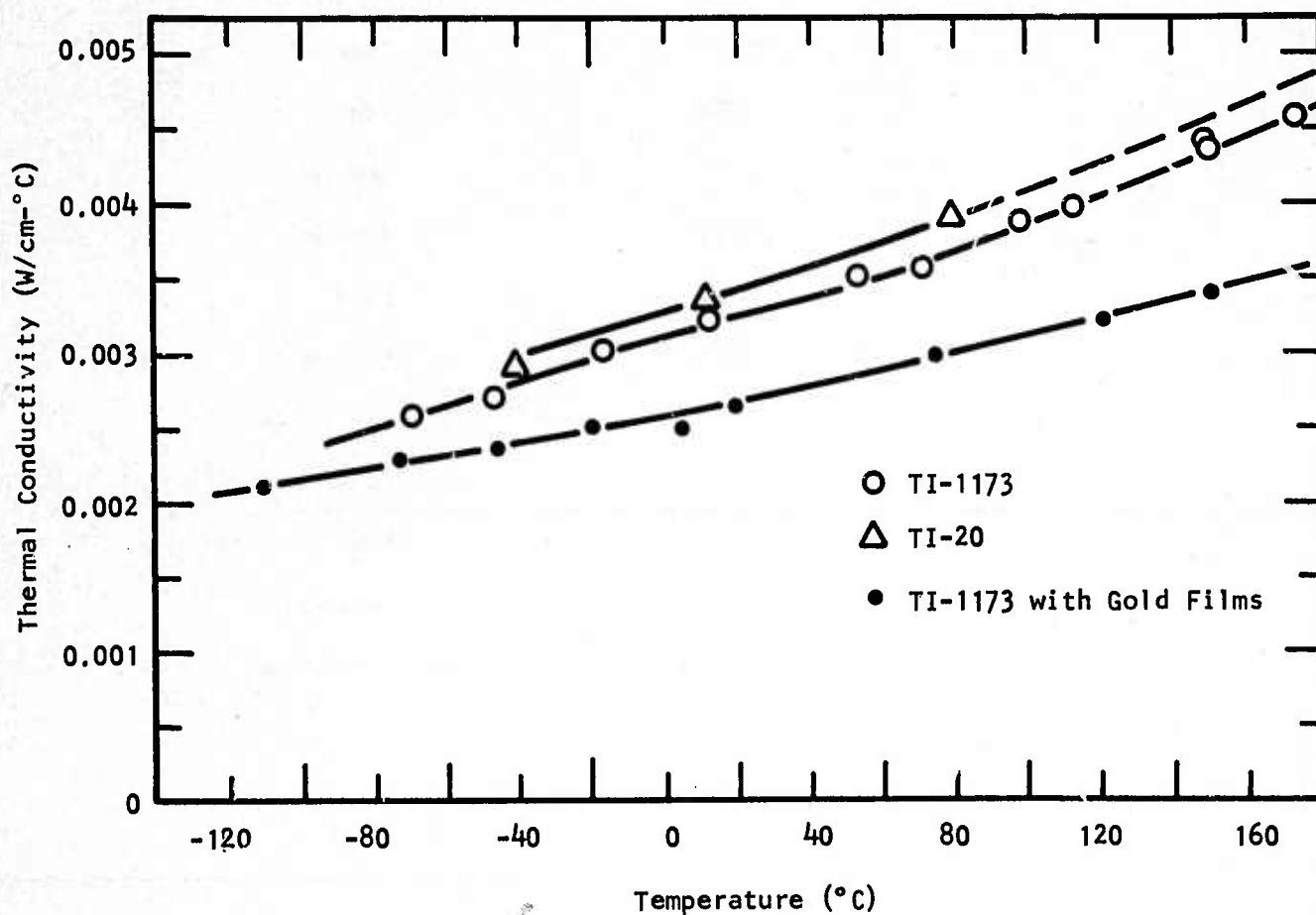
Figure 27 Measured Thermal Conductivity of TI-1173 and TI-20 as a
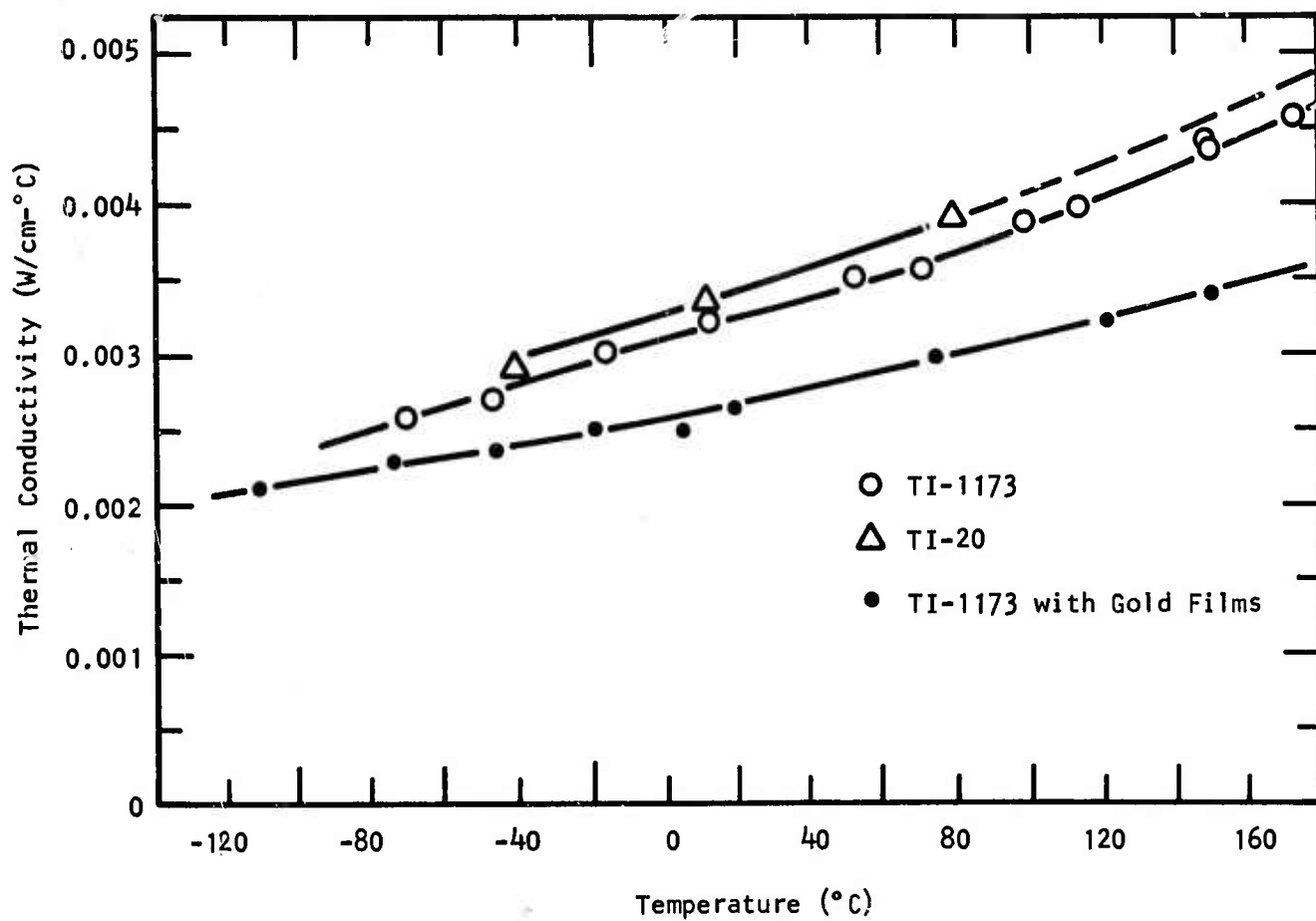Function of Temperature

59

Figure 27   Measured Thermal Conductivity of TI-1173 and TI-20 as a
Function of Temperature

59

TABLE V

MEASURED RUPTURE MODULUS OF TI-1173

Sample	Rupture Modulus	Fracture Origin
1	3128	Bottom Surface
2	2202	Side
3	3567	Edge
4	2794	Bottom
5	3334	Bottom
6	2634	Edge
7	3533	Bottom
8	3245	Indeterminate
9	2912	Edge
10	2787	Edge
11	3328	Bottom
12	2870	Indeterminate

The experimental difficulty associated with the rupture modulus measurement is evident from the large number of edge failures listed in Table V. The flaw condition at the edges of the bars tends to be more severe as a result of the cutting operation than the conditions existing on the plane surfaces. To escape the edge effect and test only the surface, it was decided to break large plates of cast and polished TI-1173 (plates that had failed striae or MTF tests).

A schematic of the apparatus used in testing the large $5\frac{1}{2}$ inch diameter plates is shown in Figure 28. Two semicircular rings were machined into two steel plates. A hole was drilled into the bottom plate for strain gauge leads. A ball joint was used on the top plate to insure proper alignment so that the load would be applied uniformly to the plate. The stresses developed on the bottom plate can easily be calculated using the thick plate approximation. The calculations show that the maximum stress is constant within the area of the small ring. Figures 29(a) and 29(b) are photographs taken after two plates were broken. The value of rupture modulus obtained on three samples are 1703 psi, 1611 psi, and 2434 psi. These results emphasize that as the area of the glass tested increases, the probability of including a major flaw increases. Since the grinding and polishing of these plates occurred in the glass production area, the quality was not as good as that attained in the optics department of Texas Instruments. The true strength of any infrared optical element made from any material is obtained only when samples have been ground and polished in the same way they will be in use. Special treatments to produce high rupture modulus values in the laboratory are only misleading.
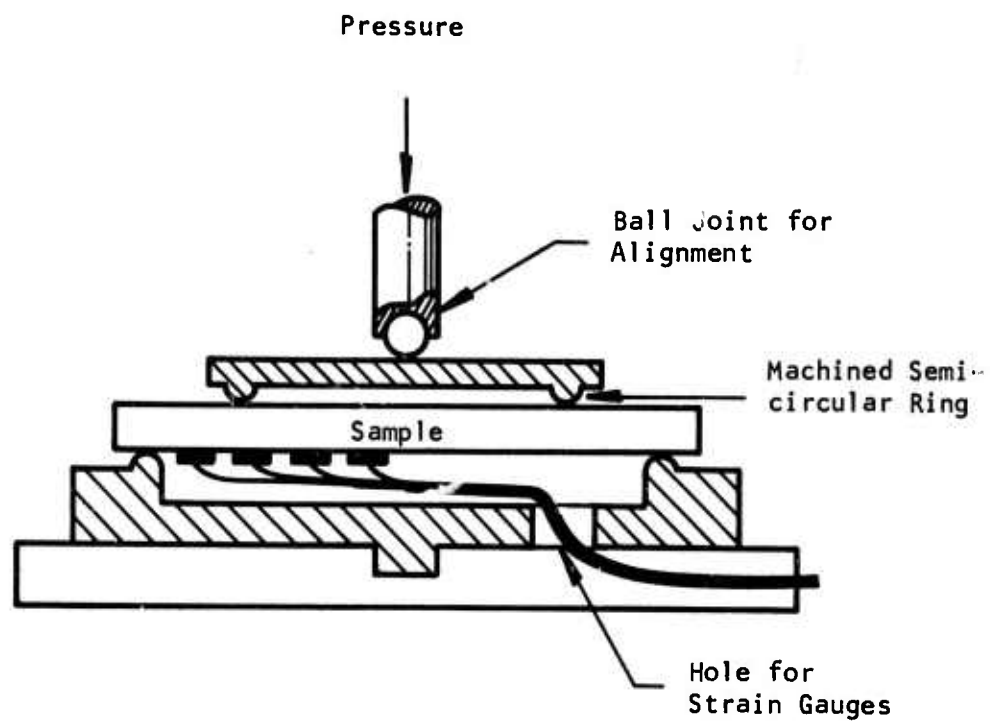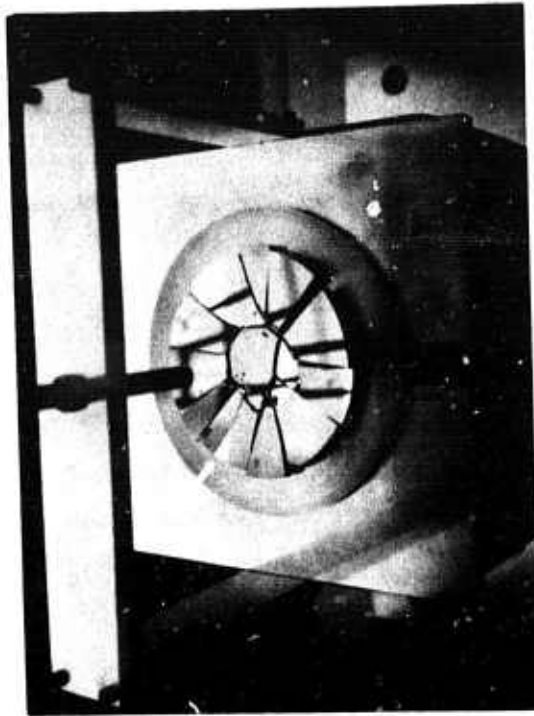
Figure 28   Apparatus Used to Test Large Circular Cast
Glass Plates

Picture Taken Immediately After Fracture,
5.5 in. Diameter, 0.5 in. Thick

With Top Plate Removed,
5.5 in. Diameter, 0.25 in. Thick

Figure 29   Photographs of Glass Plates After Fracture

SECTION VI

CONCLUSIONS

A. Selenium-Based Glasses

1. The magnitude of the absorption coefficient at 10.6 μm in the Ge-Sb-Se glass TI-1173 at the present state of purity is about 0.01 cm^{-1}. The value is limited by the concentration of "silica" in the glass. Removal of this impurity and the associated absorption should reduce the magnitude of the absorption coefficient to the 0.001 to 0.005 cm^{-1} range. The absorption at 10.6 μm below this range is determined by a broad, low-level absorption (0.2 cm^{-1}) centered about 13.4 μm. The absorption appears to be intrinsic.

2. The magnitude of the absorption at 10.6 μm in the Ge-As-Se glass TI-20 at the present state of purity is about 0.05 cm^{-1}. The value is limited by a broad, low-level absorption (0.35 cm^{-1}) centered about 12.8 μm. The absorption appears to be intrinsic.

3. The broad, low-level absorption occurring around 13 μm in Ge-Sb-Se and Ge-As-Se glasses shows a temperature dependence for absorption that indicates a third-order process. The exact origin of the band at this time is not known.

B. Interdependence of Physical Parameters

1. Compared to selenium-based glasses, the sulfur-based glasses are less dense, have higher glass transition temperatures, lower volume expansion, larger elastic moduli, greater hardness, and higher thermal conductivity. The strength of the glass, as for all brittle materials, depends on the size and quantity of defects introduced in the surface during the polishing process.

2. On the basis of the physical parameter data presented in this report, if one were free to change completely to sulfur base, considering only the physical properties, the resulting glass should be harder (+30%) and should have increased elastic moduli (+25%), increased thermal conductivity (+40%),

an increase in glass transition temperature (+10%), and a decrease in volume expansion. The degree to which the increase in physical properties can be realized will depend on the absorption at 10.6 μm and the thermal stability of the melt-formed glass.

SECTION VII

FUTURE WORK

A. Sulfur-Based Glasses

Selection of specific glass compositions to be made in large quantities for detailed evaluation will be the major emphasis in the remaining portion of the program. Guidance will come from the physical parameter interdependence data and from specific results obtained from small glass samples prepared from the Ge-S, Ge-As-S, Ge-Sb-S, or other sulfur-based systems. Choices will be based first on absorption by constituent elements, the electronic absorption edge wavelength (in order to obtain $\Delta N/\Delta T = 0$), and thermal stability of the glass. The physical properties of the small glass samples will be estimated with the aid of sound velocity measurements and the dilatometer measurement. Great care will be exercised in purifying starting reactants and avoiding the confusion of impurity absorption.

B. Selenium-Based Glasses

Preparation of TI-1173 that is free of silica will be attempted once more. Efforts will continue to establish the origin of the band around 13 μm in Ge-Sb-Se and Ge-As-Se glasses.

REFERENCES

1. W. Kaiser and P. H. Keck, J. Appl. Phys. 28, 882 (1957).

    W. Kaiser, P. H. Keck, and C. F. Lange, Phys. Rev. 101, 1264 (1956).

2. A. Vasko, D. Lezal, and I. Srb, J. Non-Cryst. Sol. 4, 311 (1970).

3. E. A. Schweikert and H. L. Rook, Anal. Chem. 42, 1525 (1970).

4. M. Hass, Naval Research Laboratory, "High Energy Laser Windows," Semiannual Report No. 1, December 1972.

5. D. A. Pinnow and T. C. Rich, Appl. Optics 12, 984 (1973).

6. A. R. Hilton, H. C. Hafner, and R. L. Rasmussen, Conference on High Power Infrared Laser Window Materials, Vol. II, pp. 693-704, 1972.

7. Samples from Mr. Jack Adams, Eagle Picher Corporation, Quapah, Oklahoma.

8. C. J. Phillips, Fracture, ed. by H. L. Lebowitz, Vol. II, Chapter 1, (Academic Press, New York, 1972).

9. A. Fayet, Verres Réfract 26, 35 (1972).

10. G. Lucovsky, A. Mooradian, W. Taylor, G. B. Wright, and R. C. Keezer, Solid State Commun. 5, 113 (1967).

11. V. A. Twaddell, W. C. LaCourse, and J. D. Mackenzie, J. Non-Cryst. Sol. 8, 831 (1972).

12. J. Tauc and A. Menth, J. Non-Cryst. Sol. 8, 569 (1972).

13. "Integrated Injection Laser-Waveguide Device," Contract N00014-73-C-0288, Office of Naval Research, Washington, D. C.

14. R. J. Patterson and M. J. Brau, "Infrared Transmitting Glasses in the Ge-Sb-Se System," Presented before the 129th Meeting of the Electrochemical Society, Cleveland, Ohio, May 2, 1966.

15. A. R. Hilton, C. E. Jones, and M. J. Brau, Phys. Chem. Glasses 7, 105 (1966).

16. Harold Hafner, "Development of Infrared Glass for Reconnaissance and Weapon Delivery," Contract F33615-72-C-1887, Air Force Avionics Laboratory, Wright-Patterson Air Force Base, Ohio.

17. K. A. Gschneider, Solid State Physics, Vol. 16, ed. by Fredrick Seitz and David Turnbull (Academic Press, New York, 1964).

18. S. Sakka and J. D. Mackenzie, J. Non-Cryst. Sol. 6, 145 (1971).

19. J. T. Krause, C. R. Kurkjian, D. A. Pinnow, and E. Sigety, Appl. Phys. Letters 17, 367 (1970).

20. L. Štouraĉ, A. Vasko, I. Srb, C. Musil and F. Strba, Czech. J. Phys. B18, 1067 (1968).

21. V. E. Schnaus and C. T. Moynihan, Mater. Sci. Engr. 7, 268 (1971).

22. C. Kittel, Phys. Rev. 75, 972 (1949).

23. A. J. Ledbetter, Phys. Chem. Glasses 9, 1 (1968).

ACKNOWLEDGMENTS